American Mineralogist, Volume 76, pages 985–1001, 1991

An experimental determination of calcic amphibole solid solution along the join tremolite-tschermakite

Moonsup Cho,* W. G. Ernst

Department of Geology, School of Earth Sciences, Stanford University, Stanford, California 94305-2115, U.S.A.

Abstract

Calcic amphiboles along the tremolite (Tr)–tschermakite (Ts) join in the system CaO-MgO-Al_2O_3-SiO_2-H_2O were synthesized at P_{fluid} = 8–21 kbar and at T = 750–900 °C. Reactions were reversed at seven P-T locations within the tschermakitic amphibole field of stability. In some experiments, natural stoichiometric end-member tremolite, for which analyses showed F and Cl to be absent, was employed as seed crystals to facilitate nucleation and growth of tschermakitic amphiboles. Synthetic amphiboles occur in various corundum-bearing assemblages that define the maximum Al content in Tr-Ts solid solutions at a given P and T. At 750–850 °C and 12–21 kbar, amphibole + corundum coexist with zoisite + H_2O (± talc, chlorite, and magnesium staurolite); at lower P, amphibole coexists with anorthite + H_2O (± chlorite, corundum, spinel, pyroxenes, and sapphirine). Amphibole + corundum + clinopyroxene + H_2O (± anorthite, forsterite, sapphirine, and garnet) are stable at 900 °C over the P_{fluid} range 12–18 kbar. These amphibole-bearing assemblages are replaced at higher P by clinopyroxene + talc + chlorite + zoisite + H_2O at 650–750 °C, and at higher temperatures by garnet + clinopyroxene + H_2O (± zoisite, orthopyroxene, and magnesium staurolite).

All condensed phases were analyzed with an electron microprobe. Pyroxenes vary significantly in total Al content (~0.1–0.5 cations per formula unit, pfu, based on 6 O atoms), whereas garnet is nearly constant in its composition, $Py_{79}Gr_{21}$. Composition of magnesium staurolite varies from 7.80 to 7.94 Si and 3.65 to 3.78 Mg cations pfu based on 46 O atoms (anhydrous formula). Synthetic amphiboles are at least ternary solid solutions and contain 4–11 mol% $Mg_7Si_8O_{22}(OH)_2$. Calcic amphiboles with Ts > about 45 mol% contain as much as 0.15 excess cations pfu based on 23 O atoms (anhydrous formula), whereas less tschermakitic ones are deficient in cation occupancy by up to 0.18 pfu. This trend is attributed to an $Al_2\square Mg_{-3}$ substitution in octahedral sites of calcium amphiboles, as is found in the 2:1 layer of clinochlore-sudoite solid solutions. Variable dioctahedral occupancy in the amphibole structure further complicates amphibole site assignment based on electron microprobe analyses.

Compositions of synthetic calcic amphiboles change systematically with P and T governed by coexisting mineral assemblages. The Ts content [= (8-Si-Na)/2] increases with T ($\partial Ts/\partial T$ = ~0.1 mol% K^{-1}) in the range 750–850 °C, but remains nearly constant at 850–900 °C. Pressure dramatically affects the Ts content of calcic amphiboles: it increases with P_{fluid} at 8–12 kbar ($\partial Ts/\partial P$ = 2–3 mol% $kbar^{-1}$), but significantly decreases at 12–21 kbar ($\partial Ts/\partial P$ = −2.5 mol% $kbar^{-1}$). Hence, the most tschermakitic amphibole, containing 60 ± 5 mol% Ts, i.e., 1.2 ± 0.1 $^{[4]}$Al, occurs at 12 kbar and 850–900 °C. This Al value is identical to that of synthetic magnesium chlorite and may represent a fundamental limit to Ts solubility in the 2:1 layer of biopyriboles. The Al content of Tr-Ts amphibole is a function of mineral assemblages as well as P and T and cannot be used to deduce physical conditions without identifying appropriate reaction assemblages.

Introduction

The Al content of calcic amphiboles in metabasites generally increases with metamorphic grade from greenschist through amphibolite to lower granulite facies (Robinson et al., 1982). Al_{tot} in hornblende of calc-alkalic plutonic rocks increases with increasing pressure in cases where a low-variance magmatic, near-solidus mineral assemblage occurs together with hornblende (Hammarstrom and Zen, 1986; Hollister et al., 1987). This P dependence of Al in hornblende has been investigated recently in the laboratory (Johnson and Rutherford, 1989; Thomas and Ernst, 1990), but few phase equilibrium data

* Present address: Department of Geological Sciences, College of Natural Sciences, Seoul National University, Seoul 151-742, Korea.

0003–004X/91/0506–0985$02.00

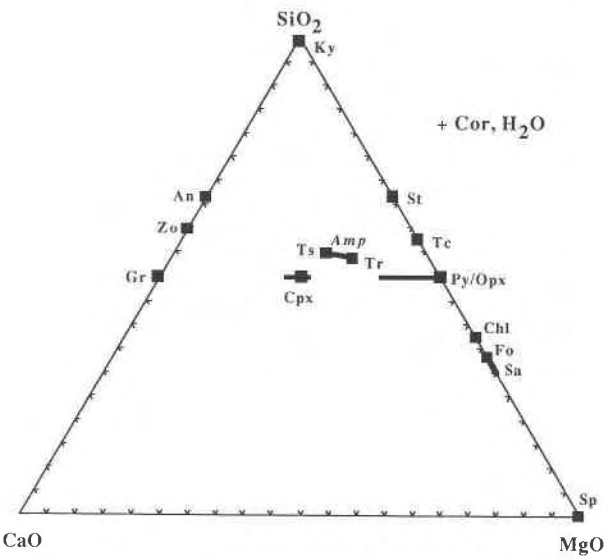

Fig. 1. Phases encountered in this study of the system CaO-MgO-Al_2O_3-SiO_2-H_2O. The diagram is a projection from Al_2O_3 and H_2O onto the CaO-MgO-SiO_2 plane in mol%. Stoichiometric end-members are illustrated by filled squares, binary solid solutions by heavy lines. Abbreviations: Amp, amphibole; An, anorthite; Chl, chlorite; Cor, Corundum; Cpx, clinopyroxene; Fo, forsterite; Gr, grossular; Ky, kyanite; Opx, orthopyroxene; Py, pyrope; Sa, sapphirine; Sp, spinel; St, magnesium staurolite; Tc, talc; Tr, tremolite; Ts, tschermakite; Zo, zoisite.

exist for calibrating the subsolidus change of amphibole composition with P and T (e.g., Spear, 1981; Pluysnina, 1982; Jenkins, 1988, 1989). This scarcity of experimental data may reflect, not only difficulty in the synthesis of amphiboles, but also the complexity of amphibole solid solutions. In addition, activity-composition relations of calcic amphiboles are poorly understood, as is apparent by the controversy concerning the existence of a miscibility gap between actinolite and hornblende or pargasite (Oba, 1980; Graham and Navrotsky, 1986; Ghent, 1988; Cho et al., 1988). In this study, we adopt a simple model system, CaO-MgO-Al_2O_3-SiO_2-H_2O (CMASH), to investigate P-T-X relationships along the join $Ca_2Mg_5Si_8O_{22}(OH)_2$(Tr)-$Ca_2Mg_3{}^{[6]}Al_2Si_6{}^{[4]}Al_2O_{22}(OH)_2$(Ts) using a piston-cylinder apparatus. Emphasis has been placed on determining compositions of Tr-Ts amphiboles synthesized with or without seed crystals of natural tremolite. Phases encountered in this study are shown in Figure 1, which is a projection from corundum and H_2O onto the CaO-MgO-SiO_2 plane.

Experimental phase equilibrium studies of tschermakitic amphiboles have been carried out by many previous workers (Jasmund and Schäfer, 1972; Oba, 1978; Cao et al., 1986; Ellis and Thompson, 1986; Jenkins, 1988). Although Oba (1978) claimed the synthesis of end-member tschermakite at 10–24 kbar and 750–850 °C, Jenkins (1988) concluded that solid solution exists only in the composition range of Ts_{00}–Ts_{50} at 12 kbar and 850 °C, decreasing to Ts_{00}–Ts_{10} at 3 kbar and 850 °C. The earlier synthesis work on the Tr-Ts join by Jasmund and Schäfer (1972) also suggested a maximum limit of the Al content in amphiboles that amounts to 55 mol% Ts at pressures of 2–10 kbar P_{fluid}. As is common in synthesis experiments of amphiboles, extremely fine grain size of experimental products hinders direct chemical analysis of tschermakitic amphiboles using the microprobe. Consequently, there are no reliable thermodynamic parameters for tschermakite and mixing properties of Tr-Ts solid solutions.

The present study aims primarily at determining the maximum Al content in Tr-Ts amphiboles over the hydrothermal P-T range of 8–24 kbar and 650–950 °C. This study first defines the upper and lower P-T limits of tschermakitic amphiboles, using five different starting mixtures with compositions in the range of Ts_{50}–Ts_{100}. The compositions of synthesized amphiboles are then investigated as a function of P, T and bulk composition.

Experimental methods

General procedures

All experiments were conducted at UCLA using a conventional piston-cylinder apparatus (Boyd and England, 1960). Further details on experimental procedures are available in Sen (1985), Cao et al. (1986), and Thomas and Ernst (1990). A furnace assembly 2.54 cm in diameter and consisting of NaCl, pyrex, graphite, BN, and MgO (Boettcher et al., 1981) was employed. Pressure was calibrated using the reaction high albite = jadeite + quartz (Johannes et al., 1971; Holland, 1980). No pressure correction for friction was required, as described by Boettcher et al. (1981). The uncertainty in pressure is estimated to be ±500 bars, including P fluctuations during an

Table 1. Compositions of five Tr-Ts amphibole starting mixtures

Starting mixture	Starting material	Compositions based on 23 O atoms					
		Si	Al	Mg	Fe	Ca	Sum
Hb	gel	7.00	2.00	4.00	—	2.00	15.00
HbC	Hb gel + natural Chl	6.91	2.10	4.11	0.002	1.92	15.04
HbX	Hb gel + natural Chl + synthetic An	6.55	2.93	3.50	0.005	2.00	14.99
HbT	natural Tr + natural Chl + synthetic An	6.28	3.44	3.31	0.02	1.94	14.99
TS	Hb gel + synthetic Chl + synthetic An	6.00	4.00	3.00	—	2.00	15.00

Note: All compositions are calculated on the basis of 23 O atoms, using the analyzed compositions of natural tremolite and chlorite (Table 2). Natural tremolite and chlorite used in the starting material are the source of trace amounts of Fe and other elements such as Na (not listed).

TABLE 2. Compositions of natural tremolite and chlorite used in the starting mixtures

	Tremolite	Chlorite		Cations based on	
	Oxide wt%			O = 23	O = 14
SiO_2	58.90 ± 0.31	29.54 ± 0.81	Si	8.014 ± 0.026	2.760 ± 0.064
TiO_2	0.02 ± 0.02	0.03 ± 0.02	Ti	0.002 ± 0.002	0.002 ± 0.001
Al_2O_3	0.08 ± 0.17	23.95 ± 0.10	Al	0.013 ± 0.028	2.638 ± 0.127
Cr_2O_3	0.02 ± 0.02	0.01 ± 0.01	Cr	0.002 ± 0.002	0.001 ± 0.001
FeO*	0.17 ± 0.03	0.48 ± 0.05	Fe	0.019 ± 0.004	0.038 ± 0.005
MnO	0.03 ± 0.03	0.01 ± 0.01	Mn	0.003 ± 0.003	0.001 ± 0.001
MgO	24.30 ± 0.18	32.13 ± 0.70	Mg	4.928 ± 0.027	4.476 ± 0.071
CaO	13.44 ± 0.08	0.01 ± 0.01	Ca	1.959 ± 0.013	0.001 ± 0.001
Na_2O	0.25 ± 0.06	n.d.**	Na	0.065 ± 0.015	0.000
K_2O	0.06 ± 0.03	0.01 ± 0.01	K	0.010 ± 0.005	0.002 ± 0.001
Total	97.26 ± 0.24	86.17 ± 0.62	Sum	15.015 ± 0.017	9.919 ± 0.012

Note: Cl and F contents in both minerals were below detection limits. One standard deviation of 12 individual analyses form several different grains are listed. Tremolite was obtained from the Stanford University Mineral Collection (SUMC 5122). Chlorite of sheridanite composition (Royal Ontario Museum Collection no. M12696) was kindly provided by John M. Allen.

* Total Fe as FeO.

** The abbreviation n.d. = not detected.

experiment (smaller than ±300 bars). In most experiments, two or three Au capsules (3 or 3.5 mm O.D.) containing different starting mixtures together with 10–20 wt% H_2O were run simultaneously. Test experiments with the same starting mixture gave identical results, not only in mineral assemblages but also in amphibole compositions. Temperatures were measured with Pt_{100}-$Pt_{90}Rh_{10}$ thermocouples placed at the top of the capsule. Temperature was maintained within ±2 °C of the experimental T using a Eurotherm controller; the uncertainty in temperature measurements is believed to be within ±10 °C. All experiments were first pressurized at room temperature to 1–2 kbar below the desired value, then heated to experimental temperature, and finally adjusted to the desired pressure. Durations of individual experiments varied from 48 to 292 h, depending on temperature; cumulative duration for reversal experiments ranged up to 330 h. Rapid quenching to room temperature was obtained by shutting off electric power to the furnace. At the conclusion of the experiments, capsules were weighed to check for weight loss, indicating possible H_2O leakage during the experiment, then punctured, and dried at 130 °C.

Starting materials

Five different starting mixtures were prepared by combining gels and crystalline phases (Table 1). The starting gel (Hb) of the Ts_{50} composition is identical to that used by Cao et al. (1986), who confirmed its stoichiometry by both X-ray fluorescence and electron microprobe techniques. Three starting mixes (Hb, HbX, and TS) lie along the join tremolite-tschermakite, but two others (HbC and HbT) contain 3 or 4 mol% $Mg_7Si_8O_{22}(OH)_2$(Cum). Excess Mg was introduced in the latter mixes in order to test the suggestion of previous workers (e.g., Wones and Dodge, 1977; Cao et al., 1986; Ellis and Thompson, 1986; Jenkins, 1987, 1988) that synthetic amphiboles are enriched in Cum component by approximately 5–10 mol%.

Natural and synthetic tremolite, chlorite, and anorthite were used as starting materials. Compositions of natural tremolite and chlorite used for preparing HbX, HbC, and HbT mixes are listed in Table 2. Both tremolite and chlorite are free of F and Cl and contain only negligible amounts of impurities such as Fe and Na. The starting anorthite was synthesized hydrothermally from an oxide mix at 700 °C and 3 kbar for 25 d. Magnesium chlorite synthesized at 669 °C and 2 kbar from an oxide mix of the clinochlore composition (sample 53 of Cho and Fawcett, 1986) was used to prepare the TS mix. The composition of this starting material, corresponding to Ts_{100}, was obtained by mixing Hb gel, synthetic clinochlore, and anorthite in a 1:1:4 ratio.

Numerous attempts were made to synthesize Tr-Ts amphibole solid solutions using either gels or oxide mixtures at low fluid pressures (≤3 kbar) in cold-seal pressure vessels. Although experiments were made within the stability field of tschermakitic amphiboles (Cao et al., 1986), the yield of synthetic amphibole was commonly less than 80%, and synthetic amphibole occurred with other phases such as pyroxenes, talc, and anorthite. A far greater yield of amphibole was obtained by introducing seed crystals of tremolite into the starting mix. It is thus apparent that amphiboles may have a smaller nucleation rate relative to other competing phases. In addition, the crystal size of amphiboles was greatly enhanced in seeded experiments, as displayed in backscattered electron images of two experimental products (Fig. 2).

Experimental charges lacking tremolite seed crystals yielded a fine-grained mixture of amphibole prisms typically less than 15 μm long and 2 μm wide. Figure 2a shows an unseeded synthetic charge (HbC2 at 12 kbar and 750 °C) in which prismatic zoisite and corundum crystals are present in an extremely fine-grained matrix of amphibole and chlorite. On the other hand, experimental charges with seed tremolite generally produced newly grown tschermakitic amphibole crystals as well as tschermakitic rims around seed tremolite (Fig. 2b). Thickness of Ts-rich rims increases from a few microme-

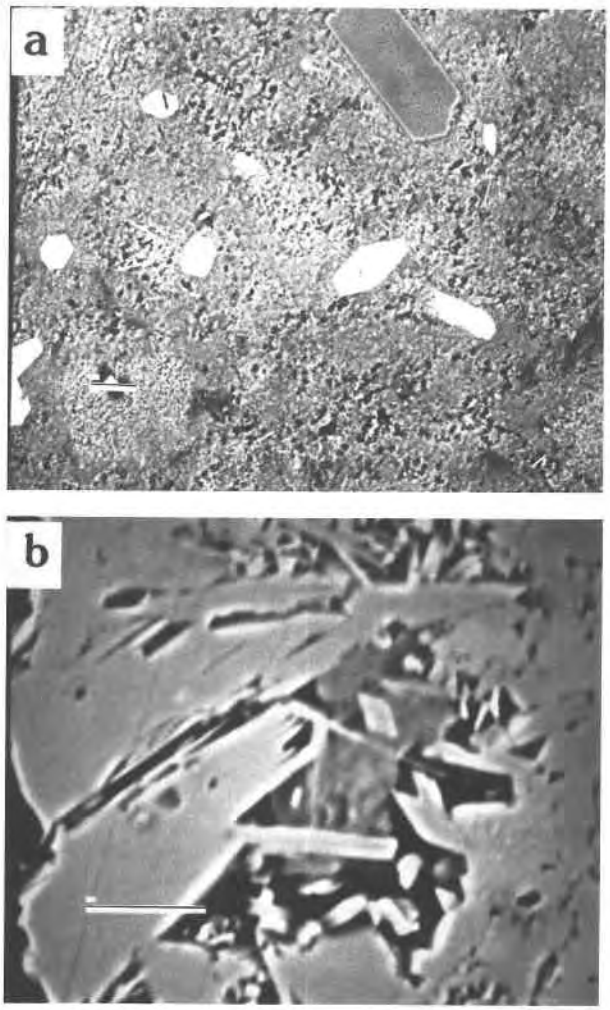

Fig. 2. Backscattered electron photomicrographs of experimental products. (**a**) A typical experimental charge containing no seed crystals of tremolite (experiment HbC2 at 12 kbar and 750 °C). Prismatic zoisite (light) and corundum (gray) crystals grow in extremely fine-grained matrix, primarily consisting of amphibole and chlorite (dark patches). Scale bar is 10 μm. (**b**) An experimental charge with seed tremolite, in which newly grown tschermakitic amphibole (Ts_{46-73}) coexists with chlorite (dark) (experiment HbT7 at 12 kbar and 850 °C). Large grains of amphibole consist of thin tschermakitic rims and Al-free cores inherited from seed tremolite crystals. Scale bar is 10 μm.

ters at low P and T to much greater than 10 μm at high P and T. Figure 2b represents a seeded experiment (HbT7 at 12 kbar and 850 °C) in which tschermakitic amphiboles (Ts_{46-73}) grew, replacing chlorite of the starting mixture. A wide range in Ts content is apparent, partly because of composite seed + overgrowth compositions.

Analytical methods

The products of each experiment were examined with the petrographic microscope and immersion oils, X-ray diffractometer (XRD), and electron microprobe. One experimental product was also examined by J. H. Ahn at Arizona State University using a high-resolution transmission electron microscope (HRTEM). Because of the fine-grained nature of most products, the identification of phases was based primarily on XRD, complemented by electron microprobe techniques. Automated XRD units with Ni-filtered, Cu$K\alpha$ radiation were used to examine smear mounts on glass slides. All mounts were scanned at 1° 2θ min^{-1} to evaluate the yield of synthetic amphiboles and to identify associated phases.

Most products obtained using the HbT starting mix show significant splitting in amphibole peaks due to the coexistence of newly grown tschermakitic amphibole and relict seed tremolite. In particular, d_{310} peaks of the coexisting amphiboles are distinct and their intensity ratios provided useful information to estimate the extent of reactions forming tschermakitic solid solutions. It is evident from intensity ratios listed in Table 3 that the maximum yield of tschermakitic amphibole occurs at 12–15 kbar P_{fluid} and 900 °C. Furthermore, the d_{310} spacing is sensitive to changes in the composition of synthetic amphibole, as determined by Jenkins (1988). For the HbT-series experiments, d_{310} of tschermakitic amphibole was measured by scanning over the region 28.4–29.0° 2θ at 0.2° 2θ min^{-1}, using d_{310} (= 3.124 ± 0.002 Å) of seed tremolite as an internal standard. The selection of tremolite as a standard is justified because compositions of seed tremolite, analyzed by electron microprobe, are identical before and after experiments throughout the P-T-time range of this study.

The d_{310} value was also measured for some tschermakitic amphibole samples synthesized from the starting mixes (Hb, HbX, and TS) lacking seed tremolite. Corundum was present in most experimental products but not at concentrations where it could be used as an internal standard. Accordingly, quartz was added to some products for this purpose. The XRD results are listed in Table 3 and shown in Figure 3, along with average Ts contents of synthetic amphiboles analyzed by electron microprobe. For most experiments, no variation in d_{310} values of newly synthesized amphiboles was detected as a function of starting material crystallinity (seeded vs. unseeded mix).

Jenkins (1988) determined that d_{310} of amphibole synthesized at 12 kbar and 850 °C decreases systematically with starting bulk compositions, ranging from Ts_{00} to Ts_{50} (Fig. 3); in contrast, he found an essentially constant d_{310} value for amphiboles synthesized from starting mixes in the compositional range of Ts_{50}–Ts_{100}. Jenkins concluded that at 12 kbar, solid solution exists near the compositional range Ts_{00}–Ts_{50} but neither precisely on nor along the entire Tr-Ts join. The result of this study is in good agreement with Jenkins' calibration when the uncertainty in his d_{310} values, ranging up to ±0.005 Å, is taken into account. We have shown (Fig. 3) that the value of d_{310} decreases with increasing Ts mol% of synthetic amphiboles where Ts <60 mol%. In conjunction with our unpublished d_{310} value of synthetic tremolite (3.119 Å), all of our data fit a second-order polynomial:

TABLE 3. Summary of experimental data

Experiment no.*	P (kbar)**	T (°C)	Duration, (h)	Remarks†	I_r (Ts/Tr)‡	$d_{310,Amp}$	Ts mol%
HbX2	7.96 ± 0.12	700	292	An > Amp ≈ Chl ≫ Cpx ≈ Tc			
HbT9	8.0 ± 0.13	750	215	Amp > Chl > An ≫ Cor	0.25	3.0982	
Hb17A§	8.0 ± 0.13	750	215	Amp ≫ An		3.105	31.1
HbT9A	8.04 ± 0.07	750	233	Amp > An > Chl > Cor(?)	0.7	3.1005	36.1
HbX8A	8.04 ± 0.07	750	233	Amp > An ≫ Cor		3.0957	45.3
HbT15	7.93 ± 0.37	850	207	Amp > An > Sp ≫ tr. (Opx + Cor)	0.5	3.096	37.8
HbX13	7.93 ± 0.37	850	207	Amp ≫ An > Sp ≥ Opx		3.097‖	45.0
HbX1	10.02 ± 0.10	651	287	An > Amp > Chl ≫ Cpx ≈ Tc > tr. Cor			
Hb19	10.02 ± 0.10	751	141	Amp ≫ An		3.096	41.2
HbX8	10.09 ± 0.17	800	114	Amp ≫ An > Cor		3.095‖	
HbT18	10.07 ± 0.27	850	206	Amp > An > Cor > tr. Sa		3.094	54.6
HbX15	10.07 ± 0.27	850	206	Amp ≫ An > tr. Cor (+ tr. unknown?)		3.0923	53.1
HbT3	12.01 ± 0.14	750	140	Amp > Cor > Zo	1.0	3.0975	41.8
HbX6	12.01 ± 0.14	750	140	Amp > Cor > Zo ≫ tr. Chl		3.099‖	
HbC2	12.01 ± 0.14	750	140	Amp ≫ Zo ≈ Chl ≈ Cor		3.099‖	
HbT3A	11.96 ± 0.16	750	144	Amp > Cor > Zo	1.5	3.0983	42.8
HbX6A	11.96 ± 0.16	750	144	Amp > Zo ≈ Cor; Chl of HbX6 absent		3.0992	35.8
HbX16A	11.96 ± 0.16	750	144	Amp ≫ An(?)		3.0929	53.8
HbT7	11.99 ± 0.07	850	115	Amp > An > Cor	0.9	3.096	59.7
HbX9	11.99 ± 0.07	850	115	Amp ≫ An ≈ Cor		3.096‖	
HbT19	12.20 ± 0.22	900	120	Amp > Cor > Cpx > tr. An	2.7	3.095	59.5
HbT20	12.20 ± 0.22	900	120	Amp > Cor ≥ Cpx ≫ tr. Sa	2.2	3.094	57.1
HbX16	12.20 ± 0.22	900	120	Amp > Cpx > Cor		3.094‖	58.4
TS1	12.20 ± 0.22	900	120	Amp > Cpx > Cor ≫ tr. Fo(?)		3.095‖	56.0
HbT26	11.92 ± 0.10	950	72	Cpx > Sp ≥ Opx (+ unknown?)			
Hb24	11.92 ± 0.10	950	72	Cpx > Opx ≫ tr. Fo (+ melt)			
HbT6	14.96 ± 0.06	750	137	Amp ≫ Cor > Zo	0.5	3.0983	51.2
HbX11	14.96 ± 0.06	750	137	Amp ≫ Cor > Zo		3.093	42.7
HbT6A	15.1 ± 0.3	750	193	Amp ≫ Zo > Cor			46.9
HbT19A	15.1 ± 0.3	750	193	Amp ≫ Zo > Cor			49.7
HbT28	15.0 ± 0.15	850	156	Amp ≫ Zo ≈ Cor	1.7	3.096	42.3
TS1A	15.0 ± 0.15	850	156	Amp > Zo > tr. Cor		3.0948	49.2
HbX18	15.0 ± 0.15	850	156	Amp ≫ tr. (Zo + Cor)		3.0960	47.9
HbT23	14.96 ± 0.05	900	93	Amp ≫ Cpx ≈ Cor	3.2	3.0945	49.5
TS3	14.96 ± 0.05	900	93	Amp ≫ Cpx ≈ Cor		3.0931	50.8
Hb17C§	14.96 ± 0.05	900	93	Amp ≫ Gt ≥ Cpx		3.0944	46.2
HbT22	17.91 ± 0.24	650	90	Chl > Tc > Zo (> metastable Tr)			
HbX17	17.91 ± 0.24	650	90	Tc > Chl > Zo ≫ Cpx			
HbT14	17.8 ± 0.24	750	113	Amp > Cor ≈ Zo ≫ Chl > tr. Ky	0.9	3.1012	28.6
HbX12	17.8 ± 0.24	750	113	Amp > Tc > Chl ≫ Zo		3.1027	31.6
HbT14A	17.54 ± 0.26	750	161	Amp ≫ Zo ≈ Cor			29.2
HbT20A	17.54 ± 0.26	750	161	Amp ≫ Zo ≈ Cor > tr. Ky			36.2
HbT16	17.8 ± 0.2	850	90	Amp ≫ Cor ≈ Zo	1.2	3.0996	49.6
HbT16A	17.82 ± 0.18	850	120	Amp ≫ Cor ≈ Zo			41.1
TS9	17.82 ± 0.18	850	120	Amp > Gt ≈ Zo > Cor		3.0947	43.2
HbT19B	17.82 ± 0.18	850	120	Amp > Gt > Cor (+ tr. relict Cpx)			49.6
HbT24	18.08 ± 0.29	900	72	Gt > Cpx ≈ Amp > Cor	1.0	3.0955	41.3
TS2	18.08 ± 0.29	900	72	Gt > Cpx > Cor (+ tr. unknown ?)			
HbT25	20.90 ± 0.3	750	117	Amp > Chl > St ≈ Zo > tr. Cor		3.107	19.0
TS4	20.90 ± 0.3	750	117	Zo > Tc > Chl			
Hb17D§	20.90 ± 0.3	750	117	Amp ≫ Chl ≥ Tc ≈ Zo		3.108‖	
HbT17	21	850	19	Amp ≫ Cor ≈ Zo ≈ quartz (?)	0.6	3.097	42.2
HbX14	21	850	19	Amp ≫ Opx ≈ Cor ≈ Zo ≥ Cpx		3.099	37.9
HbT17A	20.7 ± 0.14	850	74	Amp ≫ Cor ≈ Zo, Gt, Cpx (?)			34.6
TS10	20.7 ± 0.14	850	74	Gt > Opx > Cpx			
TS3A	20.7 ± 0.14	850	74	Amp ≫ Cor ≈ Zo ≈ Gt			33.9
HbT29	23.85 ± 0.24	850	48	Gt > Opx ≈ Zo ≈ Cpx ≈ St (+ metastable Amp)			
HbX14A	23.85 ± 0.24	850	48	Gt ≫ Cpx ≫ Opx ≈ Zo (+ tr. St, quartz?)			
Hb27	23.85 ± 0.24	850	48	Opx ≥ Cpx > Zo > Gt > tr. St			

* Each experiment number is prefixed according to the starting mixture employed. See Table 1 for further details on the starting mixture. Reversal experiments using the previous experimental product as starting material are indicated by a suffix A or B attached to the number of previous experiments.

** The listed one standard deviation refers to the P fluctuation measured during an experiment.

† Crystalline products are listed in order of decreasing intensity of their strongest characteristic XRD peaks, although the relative proportions of the phases identified could not be estimated reliably due to the preferred-orientation effect. Trace (tr.) indicates those phases that are present in small amounts detectable only by electron microprobe or optical microscope techniques.

‡ Intensity ratios of the (310) peak of newly grown tschermakitic amphibole relative to that of seed tremolite.

§ The product of Hb17 (Amp + An + Cpx + Opx), synthesized at 2 kbar, 750 °C, and 27 d, was used for experiments Hb17A to Hb17D.

‖ The d_{310} value measured without an internal standard, but believed to be accurate to ±0.003 Å.

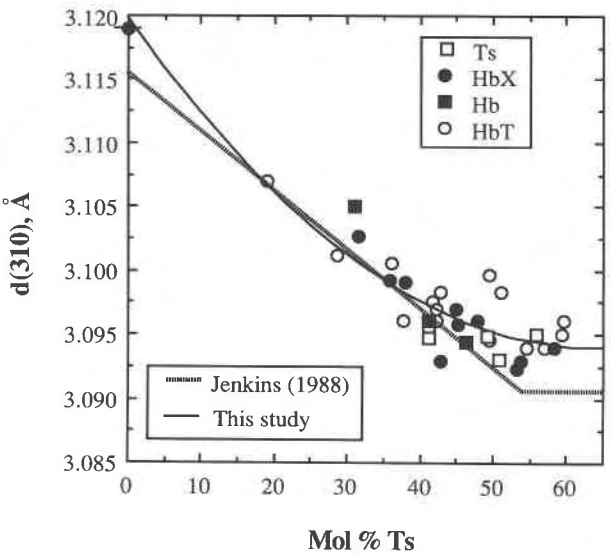

Fig. 3. Mol% Ts vs. d_{310} of calcic amphibole along the pseudobinary join Tr-Ts. Different symbols represent seeded (HbT) and unseeded (TS, HbX, and Hb) experiments, respectively. All of the data, including d_{310} value of synthetic tremolite (dot with a dash), can be described by a second-order polynomial formulation shown as the solid line. The dotted line represents the Ts-d_{310} relationship determined by Jenkins (1988). The average uncertainties (1σ) in our measurements of Ts and d_{310} values are 6 mol% and 0.001 Å, respectively. Refer to Table 4 for the standard deviation of average Ts content in each experiment.

$$d_{310} = 3.12 - 8.10 \times 10^{-4} \times \mathrm{Ts} + 6.35 \times 10^{-6} \times (\mathrm{Ts})^2,$$
$$r^2 = 0.87 \qquad (n = 34)$$

where d_{310} and Ts are in Å and mol%, respectively. This relationship is applicable only when the Ts content is less than about 65 mol%. A straight line fit is not used in order to optimize the fitting to the well-defined d_{310} values of tremolite and most tschermakitic amphiboles. Although the Ts content of synthetic amphiboles may be easily estimated by determining d_{310}, its uncertainty can be large, particularly for amphiboles with Ts content >40 mol% that display small variation in d_{310}. Further uncertainty arises from the unknown effect of other substitutions (e.g., $Al_2\square Mg_{-3}$, as will be detailed farther on) in amphibole solid solutions. Thus, inasmuch as the amphibole grains are big enough to be analyzed with the electron microprobe, we prefer to use the quantitative chemical analytical data.

Most of the experimental products were examined by electron microprobe to determine the chemical composition of amphiboles and coexisting phases. Fragments of products were mounted with epoxy on a glass slide, polished on one side, and analyzed using a Cameca electron microprobe at UCLA. Operating conditions were 15 kV acceleration voltage, 15 nA beam current, and 1–2 μm beam diameter. Amphiboles from unseeded experiments (e.g., Fig. 2a) are commonly very fine-grained, giving low analytical totals. The sizes of synthetic amphibole grains grown from mixes at high temperatures (850–900 °C) were typically greater than 15 μm long and 3 μm wide, allowing high-quality analyses. On the other hand, even for relatively low-temperature experiments, analyses of amphiboles from seeded experiments (HbT) produced excellent stoichiometries and wt% totals, although they were subject to contamination by relict seed tremolite. A large number of analyses were required, particularly at low P_{fluid} and T, to obtain a reproducible composition for tschermakitic amphiboles. Extreme care was taken to avoid amphibole grains containing fine granules of aluminous phases such as corundum, zoisite, and anorthite, which may cause an overestimate of the Ts content in amphibole. The amphibole compositions obtained from unseeded experiments at high temperatures completely overlap those obtained from the seeded experiments, corroborating the conclusion that our analytical method is internally consistent and that charges closely approached equilibrium phase compositions.

Results

Seventy experiments were performed at temperatures ranging from 650 °C to 950 °C and at pressures of 8 to 24 kbar. Experimental results are listed in Table 3; Figure 4 summarizes various mineral assemblages synthesized at each experimental condition. Synthetic amphibole occurs with other phases in all amphibole-producing experiments, including those from the slightly Mg-enriched starting compositions (cf. Jenkins, 1988). The identities and compositions of these extraneous phases vary with P, T, and bulk composition.

The phase compatibilities observed in synthesis experiments are largely divided into three amphibole-bearing assemblages, as well as others lacking amphibole (Fig. 4). At 650–850 °C and 8–12 kbar, amphibole ± corundum coexist with anorthite + H_2O (± chlorite, talc, pyroxenes, spinel, and sapphirine), but at 750–850 °C and 12–21 kbar, amphibole + corundum coexist with zoisite + H_2O (± talc, chlorite, kyanite, and magnesium staurolite). At 900 °C, amphibole + corundum + clinopyroxene + H_2O (± anorthite, forsterite, sapphirine, and garnet) are stable over the fluid pressure range 12–18 kbar. These amphibole-bearing assemblages are replaced at high pressures by clinopyroxene + talc + chlorite + zoisite + H_2O at 650–750 °C, and at higher temperatures by garnet + clinopyroxene + H_2O (± zoisite, orthopyroxene, and magnesium staurolite).

Compositions of calcic amphiboles coexisting with corundum and zoisite are defined by the simple degenerate reaction

$$3\ (\text{tremolite})_{Amp} + 2\ \text{zoisite} + 7\ \text{corundum} + H_2O = 5\ (\text{tschermakite})_{Amp}. \qquad (1)$$

This reaction relationship is shown by the pseudobinary colinearity of the Zo-Ts-Tr join in Figure 1. Six reversal experiments for Reaction 1 were conducted at 750 and 850 °C. Figure 5 shows the result of reversal experiments in terms of experiment duration and average Ts content

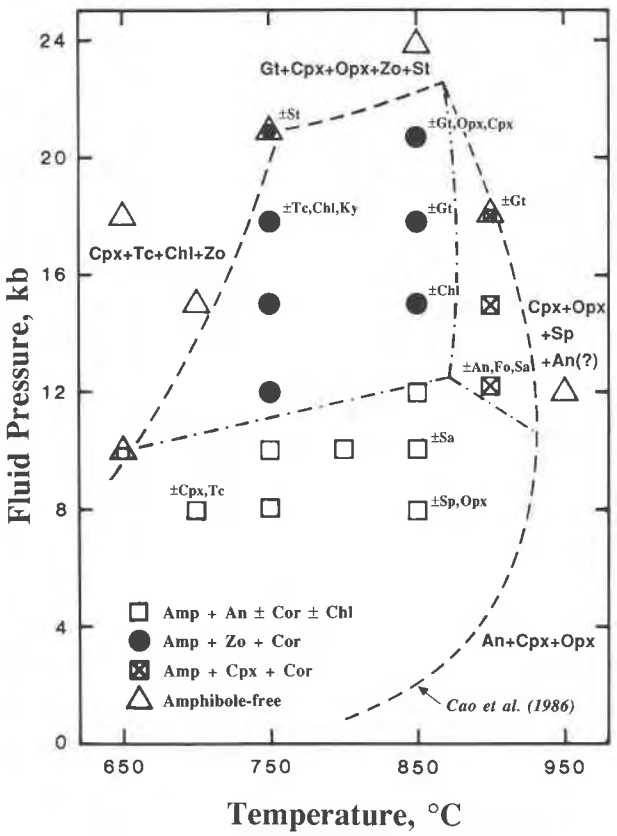

Fig. 4. P_{fluid}-T diagram illustrating various mineral assemblages synthesized at each experimental condition. When mineral assemblages vary depending on starting bulk compositions, those of aluminous starting materials (i.e., HbX, HbT, or TS mix) are shown. Dashed curves approximately define P-T limits for the stability of phase assemblages containing tschermakitic amphibole. The dot-dashed curves schematically show the boundaries between different amphibole (Amp)-bearing assemblages. Various breakdown assemblages are also shown for each amphibole-absent P-T region. The upper thermal stability of tschermakitic amphibole at low pressure is adopted from Cao et al. (1986). Abbreviations: Gt, Garnet; see the caption of Figure 1 for other abbreviations.

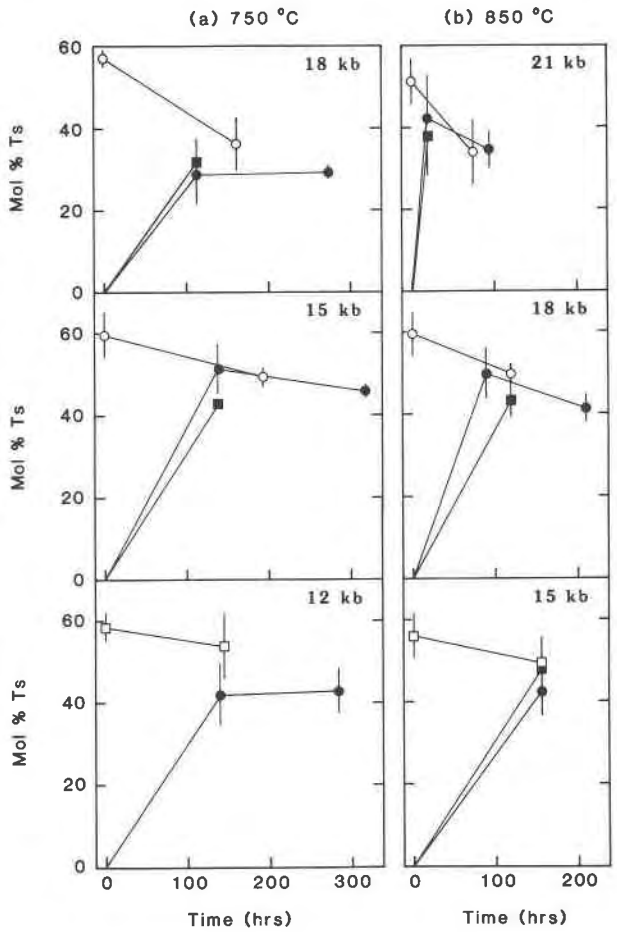

Fig. 5. Experimental time vs. mol% Ts of synthetic calcic amphibole, coexisting with corundum and zoisite (+ H_2O), in six reversal experiments at (**a**) 750 °C and (**b**) 850 °C. Open symbols are for experiments starting with products containing tschermakitic amphibole synthesized at 900 °C and 12–15 kbar; closed symbols are for those with seed tremolites or without any seed crystal of calcic amphibole. Circles and squares represent seeded and unseeded experiments, respectively. Error bars represent one standard deviation for the analyzed Ts content.

(±one standard deviation) of each experiment (Table 4). Products containing tschermakitic amphibole synthesized at 900 °C and 12–15 kbar (Table 3) were used as starting material to obtain a compositional bracket from the Al-rich side. It is apparent that Al-rich amphibole first grows metastably, converting to less aluminous amphibole with increasing duration. This observation corroborates the suggestion of Jenkins (1988) that metastable, Al-rich amphibole rapidly nucleates in the Al-rich starting mixtures and then reacts to produce aluminous phases such as Cor and An in order to more closely approach the less aluminous equilibrium composition. Similar occurrences of metastable, aluminous pyroxenes have been observed in our own and many other experiments (e.g., Danckwerth and Newton, 1978; Lane and Ganguly, 1980; Wood, 1979; Hansen, 1981; Perkins et al., 1981; Wang and Greenwood, 1988).

Reversal experiments from the less aluminous side of Reaction 1 were made from various starting mixtures with or without tremolite seed crystals (Table 3). No significant discrepancy was observed because of the difference in starting materials. It may be noted from Figure 5 that uncertainities generally decrease with increasing experiment duration, indicating progressively closer approaches toward equilibrium. The large apparent uncertainty in the Al-rich side bracket of reversal experiments results simply from the difficulty in distinguishing between seeded and newly grown tschermakitic amphibole. Systematic variation of amphibole compositions with P and T as well as chemical reproducibility of amphiboles from dif-

TABLE 4. Average compositions of analyzed amphibole in each experiment

Experiment no.	P (kbar)	T (°C)	n*	Total wt%	Si	Al	Fe	Mn	Mg	Ca	Na	K	Cation sum
Hb17A	8.0	750	7	92.9	7.37	1.34	0.00	0.00	4.31	1.93	0.01	0.01	14.97
HbT9A	8.0	750	6	95.6	7.23	1.54	0.03	0.00	4.33	1.84	0.05	0.01	15.03
HbX8A	8.0	750	5	89.3	7.09	1.95	0.01	0.00	4.04	1.84	0.01	0.00	14.94
HbT15	7.9	850	2	97.8	7.16	1.54	0.03	0.00	4.50	1.80	0.09	0.01	15.12
HbX13	7.9	850	2	81.4	7.10	1.82	0.01	0.00	4.23	1.84	0.01	0.01	15.00
Hb19	10.0	751	7	95.0	7.17	1.77	0.00	0.00	4.09	1.90	0.00	0.00	14.94
HbT18	10.0	850	7	96.4	6.87	2.13	0.03	0.00	4.14	1.87	0.04	0.00	15.08
HbX15	10.0	850	2	92.6	6.92	2.11	0.01	0.00	4.10	1.89	0.01	0.00	15.01
HbT3	12.0	750	8	94.0	7.15	1.75	0.03	0.00	4.17	1.88	0.02	0.00	14.99
HbT3A	12.0	750	8	97.3	7.11	1.77	0.03	0.00	4.16	1.91	0.03	0.00	15.02
HbX6A	12.0	750	3	94.3	7.28	1.55	0.01	0.00	4.26	1.85	0.01	0.00	14.96
HbX16A	12.0	750	16	95.6	6.92	2.11	0.01	0.00	4.10	1.89	0.01	0.00	15.04
HbT7	12.0	850	16	95.6	6.73	2.39	0.03	0.00	3.96	1.92	0.07	0.00	15.10
HbT19	12.2	900	7	95.7	6.77	2.37	0.03	0.00	3.95	1.90	0.04	0.00	15.07
HbT20	12.2	900	5	95.5	6.82	2.19	0.03	0.00	4.13	1.90	0.04	0.00	15.11
HbX16	12.2	900	10	96.2	6.83	2.30	0.01	0.00	4.03	1.85	0.00	0.00	15.03
TS1	12.2	900	15	96.1	6.85	2.20	0.01	0.00	4.10	1.87	0.03	0.00	15.06
HbT6	15.0	750	5	97.0	6.94	2.04	0.03	0.00	4.11	1.90	0.03	0.00	15.06
HbX11	15.0	750	3	89.0	7.14	1.91	0.01	0.00	3.93	1.91	0.01	0.00	14.91
HbT6A	15.1	750	6	96.1	7.03	1.90	n.a.**	n.a.	4.30	1.78	0.03	n.a.	15.04
HbT19A	15.1	750	5	97.1	6.97	2.01	n.a.	n.a.	4.14	1.90	0.04	n.a.	15.06
HbT28	15.0	850	11	96.8	7.12	1.78	0.03	0.00	4.17	1.88	0.04	0.00	15.02
TS1A	15.0	850	9	96.8	6.98	1.98	0.01	0.00	4.14	1.90	0.04	0.00	15.05
HbX18	15.0	850	19	96.7	7.04	1.94	0.01	0.00	4.11	1.88	0.00	0.00	15.00
HbT23	15.0	900	8	96.6	6.97	2.03	0.02	0.00	4.12	1.85	0.04	0.00	15.04
TS3	15.0	900	17	97.5	6.96	2.05	0.00	0.00	4.17	1.81	0.02	0.00	15.02
Hb17C	15.0	900	11	97.1	7.07	1.89	0.00	0.00	4.18	1.83	0.01	0.00	14.99
HbT14	17.8	750	8	95.7	7.40	1.35	0.03	0.00	4.27	1.86	0.03	0.00	14.95
HbX12	17.8	750	4	97.3	7.35	1.38	0.01	0.00	4.31	1.89	0.01	0.00	14.97
HbT14A	17.5	750	11	96.2	7.37	1.36	0.03	0.00	4.28	1.90	0.04	0.00	14.97
HbT20A	17.5	750	10	95.9	7.24	1.59	0.02	0.00	4.23	1.87	0.04	0.01	14.99
HbT16	17.8	850	6	95.4	6.97	2.01	0.04	0.00	4.19	1.79	0.04	0.00	15.04
TS9	17.8	850	5	96.1	7.12	1.87	n.a.	n.a.	4.15	1.81	0.02	n.a.	14.96
HbT16A	17.8	850	11	96.0	7.11	1.80	0.03	0.00	4.22	1.83	0.04	0.00	15.01
HbT19B	17.8	850	13	96.7	6.97	2.02	0.02	0.00	4.12	1.89	0.04	0.00	15.04
HbT24	18.1	900	8	97.1	7.12	1.76	0.03	0.00	4.28	1.79	0.05	0.00	15.03
HbT25	20.9	750	3	96.5	7.58	0.96	0.03	0.01	4.49	1.85	0.04	0.00	14.96
HbT17	21.0	850	7	96.0	7.12	1.73	0.03	0.00	4.30	1.82	0.04	0.00	15.04
HbX14	21.0	850	3	94.2	7.24	1.60	0.01	0.00	4.42	1.69	0.00	0.00	14.96
HbT17A	20.7	850	9	96.6	7.27	1.53	0.03	0.00	4.31	1.81	0.04	0.00	14.99
TS3A	20.7	850	12	97.3	7.32	1.36	0.00	0.00	4.47	1.82	0.01	0.00	15.00
HbT29	23.9	850	1	96.3	7.38	1.27	0.03	0.01	4.51	1.78	0.04	0.01	15.01

Note: One standard deviations (1σ) estimated from individual spot analyses of each sample are listed.
* The abbreviation n = number of analyses.
** The abbreviation n.a. = not analyzed.

ferent starting mixtures indicate a close approach to the stable phase assemblage. In addition, the reversed compositions of amphiboles document the equilibrium configuration.

Only a few attempts were made to define and reverse the univariant P-T curves bounding the observed phase assemblages. Instead, we tried to delineate the stability range of phase assemblages containing Tr-Ts amphibole solid solutions, as approximately defined by the dashed curves of Figure 4. Taken in conjunction with the experimental result of Cao et al. (1986) for the upper thermal stability limit of tschermakitic amphiboles at low pressures, it is evident that tschermakitic amphibole synthesized from Ts_{50} to Ts_{100} bulk compositions are stable over a broad P-T range. They show a wedge-like stability field diminishing with increasing pressure. At fluid pressures greater than 21–24 kbar and temperatures of 750–850 °C, tschermakitic amphibole ultimately disappears. The high-pressure boundary for tschermakitic amphibole was reversed at 23.8 kbar and 850 °C in HbX14A, which gave the amphibole-free assemblage, Gt + Cpx + Opx + Zo + St + H_2O, identical to that of synthesis experiment (HbT29). This result is in contrast with that of Oba (1978), who reported tschermakitic amphibole (+ Gt + Cpx ± Opx) at 24 kbar and 800–850 °C.

The low-T stability limit of tschermakitic amphibole is defined by the appearance of the amphibole-free assemblage, Cpx + Tc + Chl + Zo, at temperatures of 650–700 °C and pressures of 10–18 kbar. These P-T estimates are compatible with those determined at pressures below 10 kbar by Cao et al. (1986) for the appearance of a low-T assemblage, Cpx + Tc + Chl + An, at the expense of tschermakitic amphibole (+ An + H_2O).

It should be emphasized that boundary curves delimiting the occurrence of tschermakitic amphibole are multivariant because of compositional variations of some of the phases involved in the breakdown reactions. Moreover, the stability field of tschermakitic amphibole shown

TABLE 4—*Continued*

Ts (mol%)	Cum (mol%)	Sud (mol%)	Tr (mol%)
31.1 ± 5.8	3.7 ± 3.3	4.4 ± 3.8	60.5 ± 3.7
36.1 ± 11.4	8.0 ± 3.3	2.5 ± 10.8	50.9 ± 18.6
45.3 ± 3.3	8.2 ± 2.4	6.8 ± 5.2	39.5 ± 9.6
37.8 ± 9.6	10.2 ± 4.5	−2.8 ± 1.1	50.6 ± 15.7
45.0 ± 2.5	8.0 ± 0.2	0.6 ± 2.2	46.1 ± 0.1
41.2 ± 7.3	4.9 ± 3.6	6.1 ± 5.7	47.7 ± 11.2
54.6 ± 10.2	6.5 ± 2.0	−4.5 ± 6.1	41.7 ± 6.0
53.1 ± 9.5	6.1 ± 0.7	−0.1 ± 6.8	40.6 ± 1.8
41.8 ± 8.6	6.2 ± 4.9	2.9 ± 6.9	48.2 ± 7.7
42.8 ± 5.6	4.6 ± 1.7	1.2 ± 2.7	49.7 ± 4.5
35.8 ± 11.1	7.6 ± 4.7	5.2 ± 0.4	51.0 ± 13.2
53.8 ± 8.1	5.6 ± 2.5	−2.6 ± 6.4	42.9 ± 4.3
59.7 ± 12.2	3.8 ± 2.7	−3.9 ± 8.6	35.9 ± 7.1
59.5 ± 5.4	5.0 ± 1.3	−2.4 ± 5.2	35.8 ± 7.1
57.1 ± 2.1	5.1 ± 2.3	−6.8 ± 1.4	42.4 ± 3.1
58.4 ± 3.5	7.4 ± 1.7	−2.2 ± 3.2	36.3 ± 3.0
56.0 ± 5.5	6.7 ± 1.7	−3.1 ± 3.0	39.2 ± 4.5
51.2 ± 6.3	5.1 ± 2.6	−2.3 ± 4.0	44.4 ± 4.2
42.7 ± 0.4	4.5 ± 3.9	9.8 ± 4.6	42.8 ± 0.7
46.9 ± 1.6	11.2 ± 6.2	−0.4 ± 3.2	40.8 ± 7.2
49.7 ± 2.2	5.2 ± 0.6	−1.0 ± 2.0	44.3 ± 1.7
42.3 ± 5.2	6.0 ± 1.8	2.5 ± 5.3	47.3 ± 4.9
49.2 ± 6.1	5.1 ± 1.9	−0.7 ± 3.2	44.7 ± 4.8
47.9 ± 4.4	5.9 ± 1.8	1.1 ± 1.8	44.8 ± 3.8
49.5 ± 2.2	7.4 ± 1.2	0.7 ± 1.3	40.3 ± 3.1
50.8 ± 5.2	9.4 ± 1.4	−0.1 ± 2.1	38.7 ± 4.5
46.2 ± 7.7	8.6 ± 2.1	1.9 ± 1.8	42.9 ± 7.4
28.6 ± 7.5	7.2 ± 3.6	8.6 ± 3.4	54.1 ± 7.8
31.6 ± 5.7	5.4 ± 3.3	5.1 ± 4.1	57.3 ± 6.0
29.2 ± 1.9	5.2 ± 3.9	7.4 ± 3.6	56.3 ± 4.8
36.2 ± 3.5	6.6 ± 3.5	5.3 ± 4.9	50.1 ± 8.8
49.6 ± 6.1	10.3 ± 3.5	−0.6 ± 1.9	39.0 ± 7.4
43.2 ± 4.5	9.6 ± 2.7	5.9 ± 2.7	40.3 ± 7.4
41.1 ± 3.8	8.5 ± 3.7	4.0 ± 3.9	42.7 ± 8.1
49.6 ± 2.2	5.5 ± 1.1	−0.4 ± 2.2	43.2 ± 3.4
41.3 ± 4.0	10.8 ± 1.8	3.0 ± 1.9	42.4 ± 8.7
19.0 ± 2.4	7.4 ± 4.9	8.0 ± 4.1	63.6 ± 3.8
42.2 ± 10.5	9.0 ± 4.4	0.4 ± 3.7	46.5 ± 9.8
37.9 ± 10.7	15.5 ± 2.1	4.2 ± 5.7	42.2 ± 8.0
34.6 ± 4.7	9.3 ± 3.7	5.2 ± 3.6	49.0 ± 5.4
33.9 ± 8.4	8.8 ± 1.3	1.4 ± 2.5	55.9 ± 6.9
29.1	10.9	3.1	54.9

in Figure 4 is applicable only to an SiO_2-undersaturated system whose bulk composition ranges from Ts_{50} to Ts_{100}. Synthetic amphibole occurs with various corundum-bearing assemblages, defining the maximum Al content in Tr-Ts solid solutions at a given set of physical conditions. These tschermakitic amphiboles will be less stable in SiO_2-saturated bulk compositions. In addition, the coexistence of amphibole with other aluminous phases suggests that the compositions of amphiboles are less tschermakitic than those of the bulk compositions. This inference is verified by direct chemical analyses of synthetic amphiboles, as described in the next section.

Mineral chemistry

Among the minerals produced in experiments on the Ts_{50}–Ts_{100} bulk compositions, corundum, zoisite, and anorthite are essentially pure and represent nearly stoichiometric end-member compositions. Chlorite in the experimental products show a composition virtually identical to that of the starting material (Table 2). Orthopyroxene, garnet, magnesium staurolite, sapphirine, and talc show minor compositional variations. However, the compositions of amphiboles and clinopyroxene significantly change with P_{fluid} and T. Emphasis in this work has been placed on amphibole compositional variations.

Amphibole

Solid solutions. Synthetic amphiboles are at least ternary solid solutions and show wide compositional variations primarily because of three independent intracrystalline exchange components (Thompson et al., 1982) represented by the tschermakitic ($^{[6]}Al^{[4]}AlMg_{-1}Si_{-1}$), sudoitic ($^{[6]}Al_2{}^{[6]}\square Mg_{-3}$ = Sud), and cummingtonitic ($CaMg_{-1}$ = Cum) substitutions. Very minor substitutions such as $^{A}Na^{[4]}Al^{A}\square_{-1}Si_{-1}$ (= Ed) are present because of Na and Fe trace components in natural seed tremolite and chlorite.

Sudoitic substitution in amphibole is newly defined in this study by analogy with the di/trioctahedral exchange in the sixfold coordinated sites of the talc-like 2:1 layer in clinochlore [$Mg_5{}^{[6]}AlSi_3{}^{[4]}AlO_{10}(OH)_8$] and sudoite [$Mg_2{}^{[6]}\square{}^{[6]}Al_3Si_3{}^{[4]}AlO_{10}(OH)_8$] (Fransolet and Schreyer, 1984). We have experimentally demonstrated the significant role of sudoitic substitution in tschermakitic amphibole solid solutions. Compositions are described in terms of (hypothetical) end-member components: Ts, Sud, Cum, and Tr (Table 4). Their mole fractions were calculated from the number of cations on the basis of 23 O atoms pfu (anhydrous formula), following the simplified scheme: $X_{Ts} = (8 - Si - Na)/2$; $X_{Sud} = (Al - Na - 4X_{Ts})/2 = Si - 8 + (Al + Na)/2$; $X_{Cum} = (2 - Ca)/2$; and $X_{Tr} = (8 + Ca - Si - Al - Na)/2$. Note that this calculation scheme is applicable only to the CMASH system containing negligible Na or Fe content.

Tschermakitic substitution. Total and tetrahedral Al contents of amphiboles synthesized at 750, 850, and 900 °C, respectively, are plotted in Figure 6. Tetrahedral Al is calculated as the difference between 8.0 cations and the number of Si cations, assuming that tetrahedral sites are fully occupied. The majority of synthetic amphiboles contain 1.0 to 2.6 total Al cations, which corresponds to 25–65 mol% Ts for stoichiometric Tr-Ts solid solutions. No compositional gap was found in our synthesis of tschermakitic amphiboles, in contrast to a solvus between tremolite and pargasite [$NaCa_2Mg_4Al_3Si_6O_{22}(OH)_2$] experimentally determined by Oba (1980). The variation in Ts contents with P and T will be discussed in a subsequent section.

The compositional trend of the CMASH amphiboles synthesized with other aluminous phases (Cor, Zo, An, and Chl) apparently does not lie along the binary, stoichiometric join connecting tremolite and tschermakite end-members (Fig. 6). The least squares–fitted line for all data points is

$$^{[4]}Al = 0.57\ Al_{tot} - 0.12, \qquad r^2 = 0.94 \qquad (n = 388).$$

The number (n) of amphibole data is so large that the exclusion of some outliers at Al-rich compositions hardly

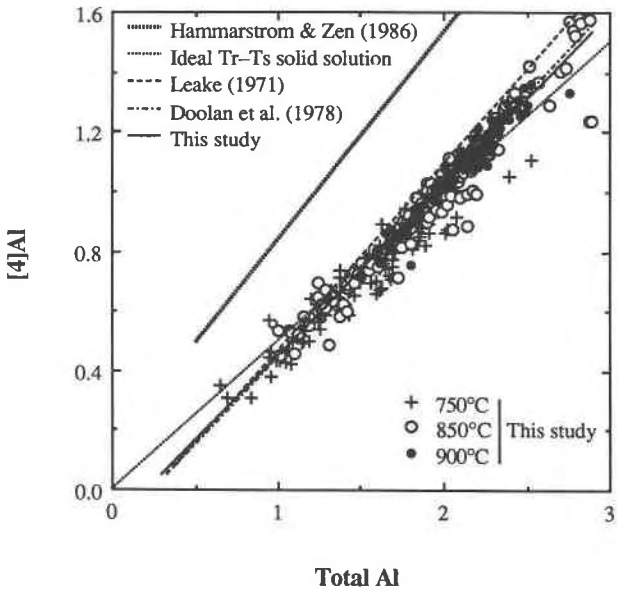

Fig. 6. Tetrahedral Al plotted against total Al of calcic amphibole samples synthesized at 750, 850, and 900 °C, respectively. Precisions of individual spot analyses are smaller than the size of symbol. Short-dashed and dot-dashed lines defining the possible limits of maximum Al contents in natural calcic amphibole are from Leake (1971) and Doolan et al. (1978), respectively. Compositional trend of hornblendes from five calc-alkalic plutonic complexes determined by Hammarstrom and Zen (1986) is also shown as the heavy dotted line. The regression line of this study is illustrated in the solid line. The thin dotted line denotes the ideal Tr-Ts solid solution.

affects the estimated slope in Figure 6. The departure from the stoichiometric composition ($^{[4]}Al = 0.5\ Al_{tot}$) is attributed to the sudoitic substitution in tschermakitic amphiboles: positive Sud exchange in Ts-rich amphiboles results in excess Al_{tot} ($^{[6]}Al > {}^{[4]}Al$), whereas negative Sud in tremolitic amphiboles yields deficient Al_{tot} ($^{[6]}Al < {}^{[4]}Al$). Similar deviation is also apparent in the compositional lines that define the possible limit of maximum Al contents in natural calcic amphibole described by Doolan et al. (1978) and Leake (1971); slopes of their lines in the plots of $^{[4]}Al/Al_{tot}$ are 0.59 and 0.62, respectively. Clearly, synthetic amphiboles plot beyond these limits, but the compositional trend is virtually identical to that of most Al-rich natural amphiboles.

Hammarstrom and Zen (1986) analyzed compositions of natural calcic amphiboles in a common magmatic mineral assemblage (plagioclase, hornblende, biotite, potassium feldspar, quartz, sphene, magnetite or ilmenite, ± epidote) from five calc-alkalic plutonic complexes from both low- and high-P regimes. In spite of large compositional variations, ranging from magnesiohornblende through edenite to pargasite, they found a tightly clustered trend,

$$^{[4]}Al = 0.69\ Al_{tot} + 0.15, \qquad r^2 = 0.97 \qquad (n = 272)$$

which is also shown in Figure 6. It is interesting that the trend of Na-, Fe-, and Ti-bearing natural hornblendes is similar to that of synthetic Tr-Ts amphiboles. In other words, the Al trend observed in natural amphiboles can be achieved by adding 0.33 to 0.45 $^{[4]}Al$ to that of synthetic amphiboles via the Ed and potassium edenite ($^{A}K^{[4]}Al^{A}\square_{-t}Si_{-t}$) substitutions.

The observation that Ed does not increase significantly with increasing Ts content in natural hornblende is in agreement with the thermodynamic calibration of the reaction, tremolite + albite = edenite + 4 quartz, as a function of P, T, and X_{Ed} by Graham and Navrotsky (1986). Their calculation suggests that a limited range of Tr-Ed solid solutions (X_{Ed} = 0.3–0.5) is in equilibrium with plagioclase and quartz over a wide range of P and T. This X_{Ed} range will be further restricted for the natural calcic amphiboles detailed by Hammarstrom and Zen (1986), which formed over a small temperature interval and equilibrated with a relatively uniform plagioclase composition (andesine to oligoclase). For example, under the restricted P-T range of 2–8 kbar and 700–800 °C, X_{Ed} ranges from 0.345 to 0.40 or 0.40 to 0.485 using a constant activity of albite equal to 0.5 or 1.0, respectively (cf. Fig. 7 of Graham and Navrotsky, 1986).

We speculate from observations described above that the Sud substitution may also occur in natural calcic amphiboles. Unfortunately, the difficulty in estimating Fe^{3+} contents from electron microprobe analyses does not warrant a further attempt to determine the extent of Sud substitutions in natural amphiboles.

Sudoitic substitution. Compositions of amphiboles synthesized at temperatures of 750, 850, and 900 °C, respectively are shown in Figure 7, which is a plot of Ts mol% vs. (Fig. 7a) Sud mol% and (Fig. 7b) cation sum based on 23 O atoms pfu. A little wider scatter in Figure 7b than in Figure 7a is apparent because total cations for calcic amphiboles from seeded experiments are generally greater by about 0.05 cations than those from unseeded experiments because of minor Na and Fe components from natural seed crystals. Analytical uncertainty for the cation sum is ±0.02 cations pfu, based on replicate analyses of seed tremolite on many different microprobe setups and grain mounts.

Also shown in Figure 7 are electron microprobe analyses of synthetic tschermakitic amphiboles reported in the literature (Oba, 1978; Cao et al., 1986; Ellis and Thompson, 1986). All of these amphibole compositions except those of Oba (1978) are restricted to Ts < 45 mol%. Cao et al. (1986) used a $Tr_{50}Ts_{50}$ starting composition identical to our Hb mix, which naturally prohibits the occurrence of more Ts-rich amphiboles in the presence of other aluminous phases such as anorthite. They used the diamond substrate technique to analyze extremely fine-grained crystals of synthetic amphiboles, in contrast to our conventional electron microprobe technique. Compositional data of these two studies completely overlap each other. On the other hand, Ellis and Thompson (1986) used various starting bulk composi-

tions containing excess quartz, which significantly suppresses the Ts solubility in amphiboles. Finally, Oba (1978) reported two amphibole analyses close to end-member Ts composition, as shown in Figure 7. However, it is difficult to determine the quality of his analytical data in the absence of oxide wt% values, and the reported coexistence of garnet, clinopyroxene, and trace quartz with the two analyzed Ts-rich amphiboles contradicts chemical constraints on the amphibole composition from mass balance considerations. This apparent discrepancy may reflect the hypothesized metastable formation of Ts-rich amphiboles prior to growth of stable, less tschermakitic amphiboles.

Figure 7a suggests a negative correlation between Ts and Sud substitutions. The Sud substitution in the Tr-Ts solid solutions exhibits a significant variation, ranging from +18 to −15 mol%. Hence, the total number of cations in the amphibole also varies because of the nature of Sud substitution involving vacant octahedral sites. This relation (Fig. 7b) indicates a progressive increase in the cation sums of synthetic amphiboles with Ts content. Calcic amphiboles with Ts > 45 mol% may contain as much as 0.15 excess cations pfu, whereas less tschermakitic amphiboles are deficient in cation occupancy by as much as 0.18 pfu. Note that the extents of the maximum and minimum Sud substitutions are provided by compositional data of Oba (1978) and Cao et al. (1986), respectively. The general agreement between our compositional data and those of previous workers seems to reinforce our conclusion on the dioctahedral substitution in calcic amphiboles.

Assuming $2(OH)^-$ pfu in Tr-Ts solid solutions, we conclude from Figures 6 and 7 that the Sud substitution accounts for the observed compositional variation in synthetic amphiboles. By this exchange mechanism, octahedral vacancies may occur in calcic amphiboles analogous to the dioctahedral micas without violating crystal-chemical principles, as originally suggested by Thompson (1978). Thus, any normalization scheme for amphibole formulae, assuming a cation sum equal to 15.0, may yield misleading results for estimating the Fe^{3+} content in amphiboles. It is also important to note that the number of total cations may exceed 15.0 for Ts-rich solid solutions. These excess cations must be assigned to the A site, because the I-beam structure is essentially close-packed (Hawthorne, 1981). Consequently, a small number of Ca cations (up to 0.15) apparently may occupy the A site of amphibole structure, analogous to the occurrence of interlayer Ca cations in margarite.

Cummingtonitic substitution. The presence of the Cum component in synthetic tremolite has been observed by many previous workers (e.g., Troll and Gilbert, 1972; Wones and Dodge, 1977; Jenkins, 1987). Based on a rigorous study, Chatterjee (personal communication, 1971, to Wones and Dodge, 1977) concluded that tremolite synthesized at 750 °C contains 5–10 mol% Cum. Jenkins (1987) also suggested that synthetic tremolite is enriched in Mg content uniformly by ~10 mol% Cum substitution

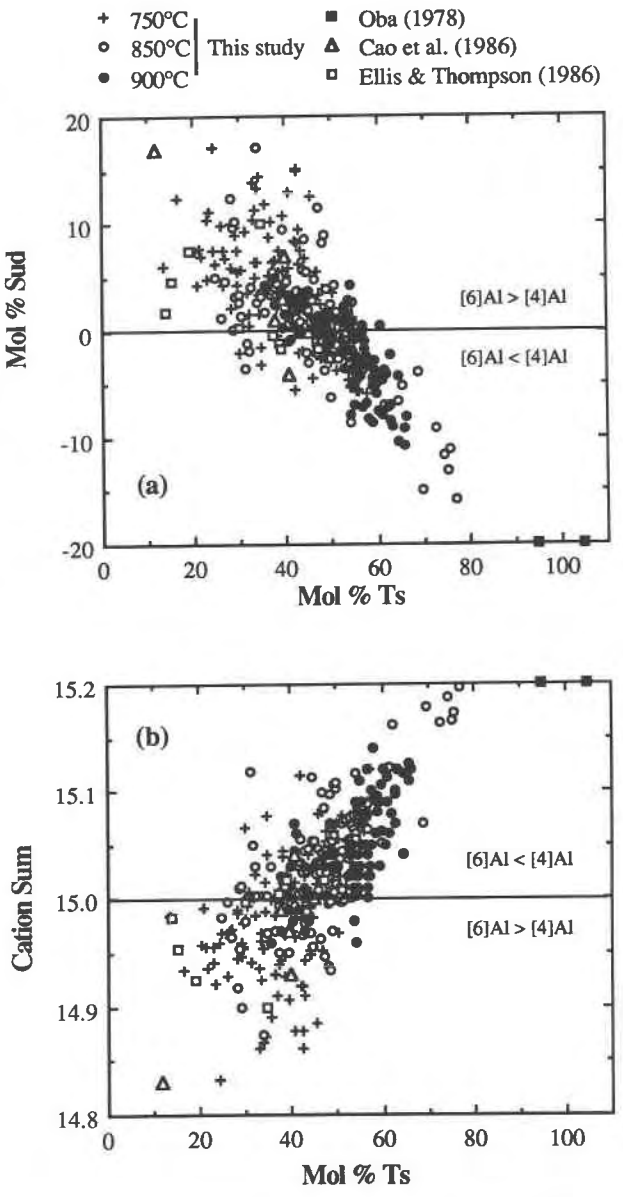

Fig. 7. Compositions of calcic amphibole samples synthesized at 750, 850, and 900 °C, respectively, plotted in terms of mol% Ts vs. (**a**) mol% Sud, and (**b**) cation sum. Typical uncertainties in mol% Ts or Sud, and cation sum of each spot analysis are 2 mol% and 0.02 cations, respectively. The solid line denotes the ideal Tr-Ts solid solution ignoring the Sud component (i.e., $^{[6]}Al = {}^{[4]}Al$). Synthetic amphibole compositions from previous works (Oba, 1978; Ellis and Thompson, 1986; Cao et al., 1986) are also shown. One tschermakitic tremolite ($X_{Ts} = 0.149$; T-1190) of Ellis and Thompson (1986) which has an exceptionally high Sud content (27.1 mol%) is not shown, because the analytical total is relatively low and the Cum content is anomalously high (18.4 mol%). If included, however, it will further strengthen the negative correlation between Ts and Sud substitutions.

over the P-T range of 6–13 kbar and 750–850 °C; however, the small grain size of synthetic tremolite did not allow him to obtain high-quality compositional data using electron microprobe techniques. Synthetic amphiboles along the join Tr-Ts are also depleted in Ca due to the Cum substitution, ranging mostly from 4 to 10 mol% (Cao et al., 1986; Ellis and Thompson, 1986; Jenkins, 1988). No previous studies, however, found any systematic change in Cum contents of synthetic amphiboles with pressure and temperature.

The average Cum content of amphibole in each experiment (Table 4) varies from 4 to 11 mol%, in good agreement with previous works. No systematic variation in Ca content was observed at low pressures ($\leq$10 kbar) or at a temperature of 750 °C. However, at higher P and T, the Cum content generally increases with both P and T. In particular, at 900 °C, the average X_{Cum} consistently increases with pressure ($\partial Cum/\partial P = 0.7$ mol% kbar^{-1}). The increase in Cum content with increasing P can be accounted for by the volume reduction accompanying replacement of Ca by Mg.

Another factor to be considered in discussing Mg enrichment in synthetic amphibole is the possible occurrence of M(4) vacancies that are typically assumed to be nonexistent in calculating Cum contents. In particular, for tschermakitic tremolite, X_{Sud} may range up to +0.15, producing 0.15 pfu of octahedral vacancies. If vacancies preferentially occur at the more highly coordinated M(4) site, rather than the smaller sixfold-coordinated M(1), M(2), or M(3) sites, the simple scheme of $X_{Cum} = (2 - Ca)/2$ may overestimate X_{Cum} by an amount of $X_{Sud}/2$, when X_{Sud} is positive. Consequently, the minimum Cum content may reach zero in amphiboles containing significant vacancies at low pressures or at 750 °C. The observed scatter at low P and T alternatively may be attributed to the occurrence of vacancies in M(4). Note that the combination of Cum and Sud substitutions is equivalent to the Eskola substitution in clinopyroxene, $\square_{0.5}AlCa_{-0.5}Mg_{-1}$ (e.g., Gasparik, 1986).

Finally, stoichiometric deviation in synthetic amphiboles may be due partly to structural disorder producing single or multiple chains in conjunction with normal amphibole double chains (Maresch and Czank, 1988). For example, Ca contents and cation sums may increase by the presence of single chains but decrease by multiple chains in structurally disordered amphiboles. The amphibole compositions of this study do not fall along the join between talc and tschermakitic clinopyroxene including biopyriboles. Structural disorder in synthetic amphibole of this study is thus inferred to be very limited in extent.

Independent evidence for limited structural disorder is obtained by examining the experimental product of an unseeded experiment at 10 kbar P_{fluid} and 751 °C (Hb19), using HRTEM. Except for the minor occurrence of triple chains, no structural disorder was found. The disordered regions in many grains of Hb19, estimated from widths in the [010] direction relative to that of double chains as a whole, seem to be less than a few percent. Hence, the effect of structural disorder on Ca and Mg compositions of amphiboles is insignificant in tschermakitic amphiboles synthesized at high pressures in this study. Although not examined with HRTEM, amphiboles from experiments seeded with tremolite, or synthesized at higher T and P than those of Hb19, are probably equally well crystallized with negligible structural disorder.

Pyroxenes

Clinopyroxene and orthopyroxene occur as thin prismatic (<300 μm) or finer stubby (<20 μm) crystals, commonly coarser than coexisting amphiboles. Both pyroxenes typically show significant variations in Al contents and less importantly, in Ca and Mg contents, suggesting that the equilibrium composition is only approximated. Some individual grain analyses are given in Table 5.[1]

The total number of Al cations based on 6 O atoms ranges from 0.14 to 0.51 pfu in Cpx, and 0.09 to 0.37 pfu in Opx. The total Al content may vary by as much as 0.22 cations pfu within one experiment (e.g., TS1). Al-rich compositions apparently fall within the compositional gap between aluminous clinopyroxene and orthopyroxene coexisting with garnet or spinel, determined by Perkins and Newton (1980) and Sen (1985), respectively. This Al enrichment is attributed to the high $\mu_{Al_2O_3}$ buffered by corundum-bearing assemblages in most experimental products of this study.

No pronounced dependence of pyroxene Al contents on P_{fluid} and T is apparent when all the data are considered. However, the Al content of Cpx coexisting with amphibole and corundum at 900 °C slightly decreases from 0.36 to 0.44 at 12 kbar to 0.32 at 18 kbar, in concert with the decreasing Ts content in amphiboles from Ts_{60} to Ts_{41} (see below). An exceptionally high Al content of 0.51, observed in HbT23 synthesized at 14.96 kbar and 900 °C (Table 5), is attributed to an overstepping of the equilibrium composition. The occurrence of Al-rich pyroxenes as metastable precursors to less aluminous pyroxenes has been commonly observed in H_2O-saturated experiments by many previous workers (e.g., Perkins et al., 1981; Wang and Greenwood, 1988).

Garnet

Garnet of the pyrope-grossular (Py-Gr) solid solution series occurs in experimental products synthesized at 15–24 kbar and 850–900 °C. It commonly grew as large euhedral to subhedral crystals ranging from 50 to 300 μm in maximum dimension, with only negligible compositional zonation (Table 5). The analyzed compositions vary from $Py_{80}Gr_{20}$ to $Py_{78}Gr_{22}$. Gr contents of these garnets are greater than the $Py_{86}Gr_{14}$ composition reported for the garnet + clinopyroxene + orthopyroxene assemblage oc-

[1] A copy of Table 5 may be ordered as Document AM-91-459 from the Business Office, Mineralogical Society of America, 1130 Seventeenth Street NW, Suite 330, Washington, DC 20036, U.S.A. Please remit $5.00 in advance for the microfiche.

curring over the *P-T* range 15–40 kbar and 900–1100 °C (Perkins and Newton, 1980). This apparent discrepancy is attributed to the more Ca-rich bulk composition investigated by us, which—at high pressures—produced calcic amphibole, clinopyroxene, and corundum in addition to garnet.

Magnesium staurolite

Euhedral laths of magnesium staurolite ranging up to 80 μm in maximum dimension occurred in three experiments at 21 and 24 kbar fluid pressure. The appearance of magnesium staurolite only at high *P* is consistent with experimental results of previous workers (Schreyer, 1968; Schreyer and Seifert, 1969; Hellman and Green, 1979). Compositions of magnesium staurolite listed in Table 5 are normalized on the basis of 46 O atoms for the anhydrous formula, to facilitate comparisons with previous compositional data (e.g., Griffen et al., 1982).

Magnesium staurolite is almost pure, with minor Fe (0.04–0.05 cations pfu) and Ca (0.01–0.02 cations pfu). Si contents range from 7.80 to 7.94 pfu, in contrast to the excess Si (8.03–8.57) in magnesian staurolite synthesized from olivine tholeiitic starting material by Hellman and Green (1979). The Si values for magnesium staurolite of this study are close to 7.74–7.92 cations pfu measured for staurolite in garnet-corundum rocks and eclogites from eastern China (Enami and Zang, 1988). The high Si values of staurolite in both synthetic and natural corundum-bearing assemblages contradicts the reasonable suggestion by Grew and Sandiford (1984) that low Si contents of staurolite reflect SiO_2-undersaturated host-rock bulk compositions.

The Mg content of staurolite synthesized in this study ranges from 3.65 to 3.78 cations pfu. These values are smaller than the sum of Fe, Mg, and Zn in any other natural magnesian staurolite except for values from two analyses reported by Grew and Sandiford (1984). Hence, our data for end-member magnesium staurolite do not support the conclusion of Enami and Zang (1988) that the Fe + Mg + Mn (+ Ti, Mn, Co, Ni, Li) content increases with increasing Mg/(Fe + Mg + Mn) ratio in staurolite.

Sapphirine

Sapphirine occurs as a minor phase in two HbT experiments and was detected only by electron microprobe techniques. Sapphirine coexists with Amp + An + Cor at 10.1 kbar and 850 °C, but with Amp + Cpx + Cor at 12.2 kbar and 900 °C. These occurrences are consistent with the stability field of the sapphirine + corundum assemblage experimentally determined by Ackermand et al. (1975).

The composition of synthetic sapphirine lies along the solid solution join between $Mg_4Al_8Si_2O_{20}$ (2:2:1 sapphirine) and $Mg_3Al_{10}SiO_{20}$ (3:5:1 sapphirine). These binary end-members are related by the tschermakitic substitution. Synthetic sapphirine of this study is close to end-member 2:2:1 sapphirine, but its content of 3:5:1 sapphirine ranges up to 13 mol% at 10.1 kbar (Table 5). In addition, the Si content of sapphirine at 12.2 kbar is slightly in excess of 2.0 based on 20 O atoms pfu. This deviation is consistent with the general tendency for natural sapphirine toward more Si-rich compositions (e.g., Schreyer and Abraham, 1975). Hence, our compositional data for synthetic sapphirine corroborate the substitution proposed by Schreyer and Abraham (1975), $Si + 0.5\square = {}^{[4]}Al + 0.5Mg$, which would produce vacant octahedral sites at higher Si contents. The occurrence of Si-rich sapphirine at high pressures in this study is also consistent with the suggestion that the 2:2:1 end-member is stable only at high *P*, whereas more aluminous sapphirine is stable at pressures less than about 7 kbar (Schreyer and Abraham, 1975; Higgins et al., 1979, and references therein).

Other phases

Talc. Talc occurs as thin euhedral plates less than 10 μm in maximum dimension and contains small amounts of Al and Ca (Table 5). Because of its fine-grained nature, microprobe analyses of talc are commonly low in oxide totals or are affected by neighboring grains, or both. However, the minor tschermakitic substitutions deduced from most analyses reported here have also been found by previous workers (Fawcett and Yoder, 1966; Newton, 1972; Evans and Guggenheim, 1988).

Zoisite. Zoisite occurs as aggregates of euhedral prisms ranging up to about 200 μm and characteristically shows typical rhombic cross sections within the fine-grained matrix of tschermakitic amphibole (Fig. 2a). Zoisite is very close to the end-member composition except for a minor Mg content, which ranges from 0.02 to 0.09 cations pfu on the anhydrous basis of 12.5 O atoms (Table 5). The occurrence of Mg in natural epidote has also been reported in low-grade metabasites (Cho and Liou, 1987).

Anorthite. Anorthite occurs as aggregates of subhedral crystals ranging up to 30–40 μm and is characteristically free of crystalline inclusions. It is close to ideal end-member composition (Table 5).

Corundum. Corundum usually forms aggregates of fine granules (<10 μm) and less commonly tabular prisms up to 50–100 μm long (Fig. 2a). No significant compositional deviation from stoichiometric Al_2O_3 was found.

Discussion

P-T dependence of Al content in tschermakitic amphiboles

The Ts-solubility limit in tschermakitic amphiboles was not well established until the reinvestigation of the Tr-Ts join by Jenkins (1988). His experimental results at 12 kbar and 850 °C indicate a solid solution existing only over the composition range Ts_{00}–Ts_{50}. Jenkins did not find any significant dependence of Ts solubility on coexisting phases (± quartz) such as corundum, anorthite, or clinopyroxene, as can be seen in his Figures 4 and 5 depicting equal Ts contents of amphiboles for various

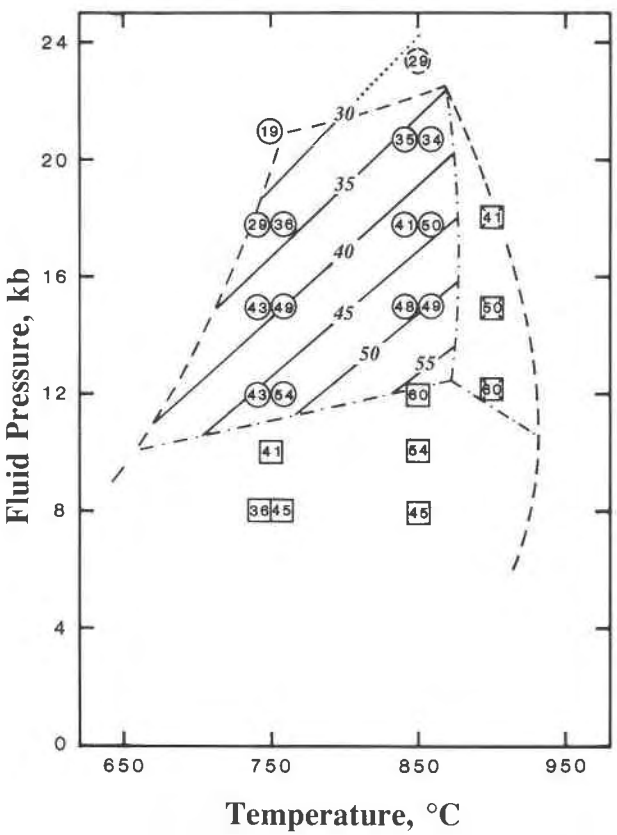

Fig. 8. P_{fluid}-T diagram illustrating isopleths for the mol% Ts of calcic amphibole in various assemblages of experimental products. For mineral assemblages and symbols, see the legend of Figure 4. Seven pairs of reversed amphibole compositions are shown at each experimental P-T condition. The maximum observed Ts content of 60 mol% (unreversed) occurs at 12 kbar and 850–900 °C. Isopleths in mol% Ts are calculated for the assemblage Amp + Zo + Cor + H_2O, assuming ideal mixing of Tr-Ts solution and the activity-composition relationship of $a_{Ts} = X_{Ts}$ (thin lines; dotted when the isopleth is metastable).

amphibole-bearing assemblages. This observation is inconsistent with the thermodynamic calculations of Leger and Ferry (1989), who showed an appreciable variation in Al contents depending solely on mineral assemblages.

Most of our experiments yielded amphibole-bearing products together with corundum at 8–21 kbar P_{fluid} and 750–900 °C. Hence, these analyses should represent the maximum Al content in Tr-Ts solid solutions under the given physicochemical conditions. We have found that compositions of tschermakitic amphiboles display systematic changes with both P and T. Solid solution relationships are shown in Figure 8 in terms of mol% Ts. The different symbols denote various amphibole-bearing assemblages as summarized in Figure 4. The compositions of amphibole were also reversed at seven different P and T locations and are shown simultaneously at each experimental condition in Figure 8.

The Ts content first increases with increasing T (∂Ts/∂T = ~0.1 mol% K^{-1}) at 750–850 °C, then remains nearly constant at 850–900 °C. Pressure dramatically affects the Ts content of calcic amphiboles: it increases with P at 8–12 kbar (∂Ts/∂P = 2–3 mol% $kbar^{-1}$), but significantly decreases at 12–21 kbar (∂Ts/∂P = −2.5 mol% $kbar^{-1}$). Hence, the most tschermakitic amphibole, containing 60 ± 5 (1σ) mol% Ts, occurs at 12 kbar and 850–900 °C. Such compositional variations are caused by the change in mineral assemblages as described below.

Compositions of calcic amphiboles coexisting with corundum and zoisite (+ H_2O), defined by Reaction 1, were reversed at six different P-T conditions (Figs. 5 and 8). Reversed compositions of the synthetic amphiboles have been used to estimate thermodynamic parameters of tschermakite; the details are to be presented elsewhere (Cho, unpublished data). The most consistent result fitting the experimental brackets was obtained by the simple activity-composition relationship of $a_{Ts} = X_{Ts}$. Calculated isopleths have gentle positive P/T slope as shown in Figure 8 and account for the observed decrease in Ts content with increasing pressure.

A similar trend of decreasing Ts content with increasing P is also evident at 900 °C and P > 12 kbar. The exact reaction governing amphibole composition varies with P, because the observed mineral assemblages (+ Amp + Cor + H_2O) change from anorthite ± sapphirine ± forsterite to clinopyroxene ± garnet. Moreover, several phases in these assemblages show significant compositional deviation from the end-members. Further studies are needed to define adequately the change in Ts content in terms of specific mineral assemblages and state variables.

On the other hand, at low P and T, the Ts content increases systematically with both P and T, buffered by various anorthite-bearing assemblages (±Cor). For example, compositions of amphiboles coexisting with anorthite and chlorite (+ H_2O) define the maximum Ts solubility at a given P and T, governed by the simple reaction

$$(\text{tremolite})_{Amp} + 8\ \text{anorthite} + 2\ (\text{clinochlore})_{Mg\text{-}Chl} = 5\ (\text{tschermakite})_{Amp} + 4\ H_2O. \quad (2)$$

One reversal of this equilibrium has been obtained at 8 kbar and 750 °C, using both tremolite and tschermakite-rich (Ts_{47} based on our d_{310}-Ts calibration) amphiboles synthesized at 10.1 kbar P_{fluid} and 800 °C (Fig. 8). Even for an experiment of 233 h, tight compositional brackets were not obtained because of sluggish reaction rates (Table 3). In conjunction with our unpublished data on the Amp + An + Chl assemblage at low pressures, synthetic amphiboles increase in Ts content with both P and T, consistent with the negative P-T slope of reaction 2 calculated based on thermodynamic data of Holland and Powell (1990).

In summary, Figure 8 shows the dependence of Ts content on mineral assemblages as well as P and T. The extent of Tr-Ts solid solution increases with fluid pressure up to approximately 12 kbar, but decreases at higher

P. Therefore, the most aluminous amphibole occurs at ~12 kbar, and the maximum Ts solubility in synthetic amphibole of the CMASH system is limited to 60 ± 5 (1σ) mol% Ts.

The solid solution series between tremolite and tschermakite is more restricted in nature, as shown by Boyd (1959), Colville et al. (1966), and Cao et al. (1986). The compilation of amphibole compositions by Cao et al. (1986) suggests that natural Tr-Ts solid solutions almost free of Fe are limited to approximately $Tr_{100}Ts_{00}$ to $Tr_{70}Ts_{30}$. However, when the $MgFe_{-1}$ substitution is taken into account, the possible Al solubility increases significantly, ranging up to about 3.0 total Al pfu, equivalent to 75 mol% Ts (cf. Fig. 1 of Cao et al., 1986).

The limited extent of solid solution observed in tschermakitic amphibole can be rationalized by examining its crystal structure, consisting principally of mica [$Mg_3Si_4O_{10}(OH)_2$] and pyroxene ($Ca_2Mg_2Si_4O_{12}$) modules (Thompson, 1978, 1981). Tschermakitic substitution occurs in both modules; however, Al is strongly ordered in the T(1) and M(2) sites, which belong to mica and pyroxene modules, respectively (Hawthorne, 1981). The tetrahedral double chains contain Al and Si in tetrahedral coordination, whereas the M(1,2,3) sites of the octahedral strip contain Mg and Al. Thus, the stability of amphibole is limited by the fit of the octahedral and tetrahedral layers analogous to other biopyriboles.

Incomplete tschermakitic substitution has been observed in other rock-forming minerals, including magnesium chlorite (Cho and Fawcett, 1986; Jenkins and Chernosky, 1986), mica (Hazen and Wones, 1972; Bailey, 1984), and orthopyroxene (e.g., Ganguly and Ghose, 1979). Synthetic magnesium chlorite along the join $Mg_6Si_4O_{10}(OH)_8$-$Mg_4Al_4Si_2O_{10}(OH)_8$ exhibits limited solid solution, reaching 1.11 to 1.20 $^{[4]}$Al in the 2:1 layer (Cho and Fawcett, 1986; Jenkins and Cheronsky, 1986). Aluminous orthopyroxenes show restricted Ts substitution to about 20 mol% following the Al-Al avoidance rule (Ganguly and Ghose, 1979). However, synthetic clinopyroxenes along the join $CaMgSi_2O_6$-$CaAl_2SiO_6$ form a complete solid solution (Gasparik, 1986). Thus, it seems likely that the maximum Ts solubility in the alkali-free calcic amphibole structure is governed by the Al substitution in the mica module or the T(1) site of the tetrahedral layer. This suggestion is further supported by agreement between the Ts-solubility limit in magnesium chlorite solid solution and the maximum tetrahedral Al content (1.2 ± 0.1) observed in synthetic tschermakitic amphiboles.

Application to natural amphiboles

The limited solid solution of synthetic amphiboles along the tremolite-tschermakite join fails to account for the high Al contents observed in natural calcic amphiboles. This discrepancy is attributed to the effect of other elements, most importantly Na and Fe in the natural system. For example, our preliminary data along the join tremolite–aluminous pargasite or sadanagaite (Schimazaki et al., 1984) indicate that the A-site of aluminous pargasite coexisting with zoisite and corundum is fully occupied by Na through the edenitic (or pargasitic) substitution. Thus, $^{[4]}$Al may range up to 2.2–2.4, which can be described by the coupled substitutions of 60–70 mol% Ts along the Tr-Ts binary join together with 100 mol% Ed along the Tr-Ed join. On the other hand, the Ed substitution in amphiboles coexisting with the common magmatic assemblage of Hammarstrom and Zen (1986) extends only to approximately 45 mol% as described earlier. Therefore, it is evident that Al contents of calcic amphiboles are a function of the coexisting mineral assemblage.

Many attempts have been made to correlate amphibole compositions with physical conditions of metamorphic and igneous processes (e.g., Spear, 1981; Laird and Albee, 1981; Hammarstrom and Zen, 1986). Recent empirical calibration of the hornblende geobarometer by Hammarstrom and Zen (1986) and Hollister et al. (1987), refined by subsequent experimental work (Johnson and Rutherford, 1989; Thomas and Ernst, 1990), has been encouraging. Our experimental results in the simple CMASH system further demonstrate that amphibole Ts content is highly dependent upon the mineral assemblage. In particular, the amphibole compositions in equilibrium with either anorthite or zoisite at 750 and 850 °C show an opposite relationship between *P* and the Ts content as described for Cor-bearing associations. Hammarstrom and Zen (1986) did not detect any effect on the Al content of hornblende due to the presence of epidote at a *P* of 8 kbar, but it is probably technically unwarranted to extrapolate linearly their empirical geobarometry to higher *P*. However, recent experimental calibration of the hornblende geobarometer by Thomas and Ernst (1990) indicates that the presence of zoisite, instead of plagioclase, at 10–12 kbar P_{fluid} does not greatly influence the Al content of hornblende in cases where the common magmatic assemblage is stable.

Nevertheless, any attempt to calibrate amphibole composition as a function of *P* and *T* should explicitly take the mineral assemblage into account. Thus, comparison of the $\partial Al/\partial P$ values of natural and synthetic amphiboles based on different assemblages (e.g., Jenkins, 1988) may be only approximately correct. Further experimental work is essential prior to applying synthetic results from simple systems to natural rocks, particularly in the absence of an internally consistent thermodynamic data set for end-members and information on the activity-composition and order-disorder relations of amphibole solid solutions.

Conclusions

1. Tschermakitic amphiboles large enough to be analyzed by conventional electron microprobe techniques were synthesized using seed crystals of natural tremolite close to end-member composition (and synthetic Ts-rich solid solutions). In addition, the high P_{fluid} ($\geq$10 kbar) of this study greatly enhanced the yield of synthetic amphi-

bole in the experiments. Characterization of one experimental product with HRTEM indicates that these synthetic amphibole samples are almost free of structural disorder except for minor proportions of triple chains.

2. Both lower and upper thermal stabilities of tschermakitic amphiboles have been approximately determined at temperatures of 650–900 °C for bulk compositions ranging from Ts_{50} to Ts_{100}. These amphiboles show a wedge-like P_{fluid}-T stability field, diminishing with increasing P; amphibole-bearing associations are replaced by eclogitic analogue assemblages at $P > 18$–24 kbar.

3. The presence of octahedral vacancies (=dioctahedral component) in synthetic amphiboles is experimentally suggested and delineated in terms of a new exchange component, $Al_2\square Mg_{-3}$. This sudoitic substitution shows a negative correlation with tscharmakitic exchange. Hence, octahedral or M(4) vacancies up to 0.18 pfu may occur in tschermakitic tremolite, whereas tremolitic tschermakite contains as much as 0.15 excess cations pfu.

4. Compositions of tschermakitic amphiboles systematically change with P and T. In particular, the Ts contents of calcic amphiboles coexisting with zoisite and corundum have been reversed at six different P–T conditions; Ts solubility significantly decreases with increasing P ($\partial Ts/\partial P = -2.5$ mol% kbar^{-1}) for the assemblage Amp + Zo + Cor + H_2O. The maximum Al content of 1.2 ± 0.1 tetrahedral Al equivalent to 60 ± 5 mol% Ts occurs at 12 kbar and 850–900 °C. The instability of more tschermakitic amphiboles is attributed to geometric constraints between tetrahedral chains and octahedral strips in biopyriboles.

Acknowledgments

Experimental and much of the analytical work on this project was done at UCLA, supported by NSF grant EAR-8616624. HRTEM and XRD of experimental products were performed at Arizona State and Stanford Universities, respectively, and the paper was written at the latter institution. Helpful and critical reviews were provided by J.B. Brady, F.C. Hawthorne, D.M. Jenkins, M.J. Rutherford, S.S. Sorensen, and W.M. Thomas. The authors are grateful to the above-named schools and scientists for their support.

References cited

Ackermand, D., Seifert, F., and Schreyer, W. (1975) Instability of sapphirine at high pressures. Contributions to Mineralogy and Petrology, 50, 79–92.

Bailey, S.W. (1984) Crystal chemistry of the true micas. Mineralogical Society of America Reviews in Mineralogy, 13, 13–60.

Boettcher, A.L., Windom, K.E., Bohlen, S.R., and Luth, R.W. (1981) Low friction, anhydrous, low- to high-temperature furnace sample assembly for piston-cylinder apparatus. Reviews of Scientific Instruments, 52, 1903–1904.

Boyd, F.R. (1959) Hydrothermal investigations of amphiboles. In P.H. Abelson, Ed., Researches in geochemistry, p. 377–396. Wiley, New York.

Boyd, F.R., and England, J.L. (1960) Apparatus for phase-equilibrium measurements at pressures up to 50 kilobars and temperatures up to 1,750 °C. Journal of Geophysical Research, 65, 741–748.

Cao, R., Ross, C., and Ernst, W.G. (1986) Experimental studies to 10 kb of the bulk composition $tremolite_{50}$-$tschermakite_{50}$ + excess H_2O. Contributions to Mineralogy and Petrology, 93, 160–167.

Cho, M., and Fawcett, J.J. (1986) The kinetic study of clinochlore and its high temperature equivalent forsterite-cordierite-spinel at 2 kbar water pressure. American Mineralogist, 71, 68–77.

Cho, M., and Liou, J.G. (1987) Prehnite-pumpellyite to greenschist facies transition in the Karmutsen metabasites, Vancouver Island, B.C. Journal of Petrology, 28, 417–443.

Cho, M., Liou, J.G., and Bird, D.K. (1988) Prograde phase relations in the State 2-14 well metasandstones, Salton Sea geothermal field, California. Journal of Geophysical Research, 93, 13081–13103.

Colville, P., Ernst, W.G., and Gilbert, M.C. (1966) Relationships between cell parameters and chemical compositions of monoclinic amphiboles. American Mineralogist, 51, 1727–1754.

Danckwerth, P.A., and Newton, R.C. (1978) Experimental determination of the spinel periodite to garnet periodite reaction in the system MgO-Al_2O_3-SiO_2 in the range 900°–1000 °C and Al_2O_3 isopleths of enstatite in the spinel field. Contributions to Mineralogy and Petrology, 66, 189–201.

Doolan, B.L., Zen, E-an, and Bence, A.E. (1978) Highly aluminous hornblendes: Compositions and occurrences from southwestern Massachusetts. American Mineralogist, 63, 1088–1099.

Ellis, D.J., and Thompson, A.B. (1986) Subsolidus and partial melting reactions in the quartz-excess CaO + MgO + Al_2O_3 + SiO_2 + H_2O system under water-excess and water-deficient conditions to 10 kb: Some implications for the origin of peraluminous melts from mafic rocks. Journal of Petrology, 27, 91–121.

Enami, M., and Zang, Q. (1988) Magnesian staurolite in garnet-corundum rocks and eclogite from the Donghai district, Jiangsu province, east China. American Mineralogist, 73, 48–56.

Evans, B.W., and Guggenheim, S. (1988) Talc, pyrophyllite, and related minerals. Mineralogical Society of America Reviews in Mineralogy, 19, 225–294.

Fawcett, J.J., and Yoder, H.S. (1966) Phase relationships of chlorites in the system MgO-Al_2O_3-SiO_2-H_2O. American Mineralogist, 51, 351–380.

Fransolet, A.-M., and Schreyer, W. (1984) Sudoite, di/trioctahedral chlorite: A stable low-temperature phase in the system MgO-Al_2O_3-SiO_2-H_2O. Contributions to Mineralogy and Petrology, 86, 409–417.

Ganguly, J., and Ghose, S. (1979) Aluminous orthopyroxene: Order-disorder, thermodynamic properties, and petrologic implications. Contributions to Mineralogy and Petrology, 69, 375–385.

Gasparik, T. (1986) Experimental study of subsolidus phase relations and mixing properties of clinopyroxene in the silica-saturated system CaO-MgO-Al_2O_3-SiO_2. American Mineralogist, 71, 686–693.

Ghent, E.D. (1988) Tremolite and H_2O activity attending metamorphism of hornblende-plagioclase-garnet assemblages. Contributions to Mineralogy and Petrology, 98, 163–168.

Graham, C.M., and Navrotsky, A. (1986) Thermochemistry of the tremolite-edenite amphiboles using fluorine analogues, and applications to amphibole-plagioclase-quartz equilibria. Contributions to Mineralogy and Petrology, 93, 18–32.

Grew, E.S., and Sandiford, M. (1984) A staurolite-talc assemblage in tourmaline-phlogopite-chlorite schist from northern Victoria Land, Antarctica, and its petrogenetic significance. Contributions to Mineralogy and Petrology, 87, 337–350.

Griffen, D.T., Gosney, T.C., and Phillips, W.R. (1982) The chemical formula of natural staurolite. American Mineralogist, 67, 292–297.

Hammarstrom, J.M., and Zen, E-an (1986) Aluminum in hornblende: An empirical igneous geobarometer. American Mineralogist, 71, 1297–1313.

Hansen, B. (1981) The transition from pyroxene granulite facies to garnet clinopyroxene granulite facies. Experiments in the system CaO-MgO-Al_2O_3-SiO_2. Contributions to Mineralogy and Petrology, 76, 234–242.

Hawthorne, F.C. (1981) Crystal chemistry of the amphiboles. In Mineralogical Society of America Reviews in Mineralogy, 9A, 1–95.

Hazen, R.M., and Wones, D.R. (1972) The effect of cation substitution on the physical properties of trioctahedral micas. American Mineralogist, 57, 103–129.

Hellman, P.L., and Green, T.H. (1979) The high pressure experimental crystallization of staurolite in hydrous mafic compositions. Contributions to Mineralogy and Petrology, 68, 369–372.

Higgins, J.B., Ribbe, P.H., and Herd, R.K. (1979) Sapphirine I crystal chemical contributions. Contributions to Mineralogy and Petrology, 68, 349–356.

Holland, T.J.B. (1980) The reaction albite = jadeite + quartz determined experimentally in the range 600–1200 °C. American Mineralogist, 65, 129–134.

Holland, T.J.B., and Powell, R. (1990) An enlarged and updated internally consistent thermodynamic dataset with uncertainties and correlations: The system K_2O-Na_2O-CaO-MgO-MnO-FeO-Fe_2O_3-Al_2O_3-TiO_2-SiO_2-C-H_2-O_2. Journal of Metamorphic Geology, 8, 89–124.

Hollister, L.S., Grissom, G.C., Peters, E.K., Stowell, H.H., and Sisson, V.B. (1987) Confirmation of the empirical correlation of Al in hornblende with pressure of solidification of calc-alkaline plutons. American Mineralogist, 72, 231–239.

Jasmund, K., and Schäfer, R. (1972) Experimentelle Bestimmung der *P-T*-Stabilitätsbereiche in der Mischkristallreihe Tremolit-Tschermakit. Contributions to Mineralogy and Petrology, 34, 101–115.

Jenkins, D.M. (1987) Synthesis and characterization of tremolite in the system H_2O-CaO-MgO-SiO_2. American Mineralogist, 72, 707–715.

——— (1988) Experimental study of the join tremolite-tschermakite: A reinvestigation. Contributions to Mineralogy and Petrology, 99, 392–400.

——— (1989) Experimental reversal of the Al content of tremolitic amphiboles coexisting with diopside, anorthite, and quartz. Geological Society of America Abstracts, 21, A157.

Jenkins, D.M., and Chernosky, J.V., Jr. (1986) Phase equilibria and crystallochemical properties of Mg-chlorite. American Mineralogist, 71, 924–936.

Johannes, W., Bell, P.M., Mao, H.H., Boettcher, A.L., Chipman, D.W., Hays, J.F., Newton, R.C., and Seifert, F. (1971) An interlaboratory comparison of piston-cylinder pressure calibration using the albite breakdown reaction. Contributions to Mineralogy and Petrology, 32, 24–38.

Johnson, M.C, and Rutherford, M.J. (1989) Experimental calibration of the aluminum-in-hornblende geobarometer with application to Long Valley caldera (California) volcanic rocks. Geology, 17, 837–841.

Laird, J., and Albee, A.L. (1981) Pressure, temperature, and time indicators in mafic schist: Their application to reconstructing the polymetamorphic history of Vermont. American Journal of Science, 281, 127–175.

Lane, D.L., and Ganguly, J. (1980) Al_2O_3 solubility in orthopyroxene in the system MgO-Al_2O_3-SiO_2: A reevaluation, and mantle geotherm. Journal of Geophysical Research, 85, 6963–6972.

Leake, B.E. (1971) On aluminous and edenitic hornblendes. Mineralogical Magazine, 38, 389–407.

Leger, A., and Ferry, J.M. (1989) High-Al hornblendes from low-P metamorphosed marls, N. Vermont, and a thermodynamic model for the Al-content of Ca-amphibole. Eos, 70, 493.

Maresch, W.V., and Czank, M. (1988) Crystal chemistry, growth kinetics and phase relationships of structurally disordered (Mn^{2+}, Mg)-amphiboles. Fortschritte der Mineralogie, 66, 69–121.

Newton, R.C. (1972) An experimental determination of the high-pressure stability limits of magnesium cordierite under wet and dry conditions. Journal of Geology, 80, 398–420.

Oba, T. (1978) Phase relationships of $Ca_2Mg_3Al_2Si_6O_{22}(OH)_2$-$Ca_2Mg_3Fe^{3+}{}_2Si_6Al_2O_{22}(OH)_2$ join at high temperature and high pressure—the stability of tschermakite. Journal of Faculty of Sciences, Hokkaido University, Series IV, 18, 339–350.

——— (1980) Phase relations in the tremolite-pargasite join. Contributions to Mineralogy and Petrology, 71, 247–256.

Perkins, D., and Newton, R.C. (1980) The compositions of coexisting pyroxene and garnet in the system CaO-MgO-Al_2O_3-SiO_2 at 900–1100 °C and high pressures. Contributions to Mineralogy and Petrology, 75, 291–300.

Perkins, D., Holland, T.J.B., and Newton, R.C. (1981) The Al_2O_3 contents of enstatite in equilibrium with garnet in the system MgO-Al_2O_3-SiO_2 at 15–40 kb and 900–1600 °C. Contributions to Mineralogy and Petrology, 78, 99–109.

Pluysnina, L.P. (1982) Geothermometry and geobarometry of plagioclase-hornblende bearing assemblages. Contributions to Mineralogy and Petrology, 80, 140–146.

Robinson, P., Spear, F.S., Schumacher, J.C., Laird, J., Klein, C., Evans, B.W., and Dooland, B.L. (1982) Phase relations of metamorphic amphiboles: Natural occurrences and theory. Mineralogical Society of America Reviews in Mineralogy, 9B, 1–227.

Schreyer, W. (1968) A reconnaissance study of the system MgO-Al_2O_3-SiO_2-H_2O at pressures between 10 and 25 kb. Carnegie Institution of Washington Year Book, 66, 380–392.

Schreyer, W., and Abraham, K. (1975) Peraluminous sapphirine as a metastable reaction product in kyanite-gedrite-talc schist from Sar e Sang, Afghanistan. Mineralogical Magazine, 40, 171–180.

Schreyer, W., and Seifert, F. (1969) High-pressure phases in the system MgO-Al_2O_3-SiO_2-H_2O. American Journal of Science, 267-A, 407–443.

Sen, G. (1985) Experimental determination of pyroxene compositions in the system CaO-MgO-Al_2O_3-SiO_2 at 900–1200 °C and 10–15 kbar using PbO and H_2O fluxes. American Mineralogist, 70, 678–695.

Shimazaki, H., Bunno, M., and Ozawa, T. (1984) Sadanagaite and magnesio-sadanagaite, new silica-poor members of calcic amphibole from Japan. American Mineralogist, 69, 465–471.

Spear, F.S. (1981) An experimental study of hornblende stability and compositional variability in amphibolite. American Journal of Science, 281, 697–734.

Thomas, W.M., and Ernst, W.G. (1990) The aluminum content of hornblende in calc-alkaline granitic rocks: A mineralogic barometer calibrated experimentally to 12 kbars. Geochemical Society Special Publication, 2, 59–63.

Thompson, J.B., Jr. (1978) Biopyriboles and polysomatic series. American Mineralogist, 63, 239–249.

——— (1981) An introduction to the mineralogy and petrology of the biopyriboles. In Mineralogical Society of America Reviews in Mineralogy, 9A, 141–188.

Thompson, J.B., Jr., Laird, J., and Thompson, A.B. (1982) Reactions in amphibolite, greenschist and blueschist. Journal of Petrology, 23, 1–27.

Troll, G., and Gilbert, M.C. (1972) Fluorine-hydrodxyl substitution in tremolite. American Mineralogist, 57, 1386–1404.

Wang, X., and Greenwood, H.J. (1988) An experimental study of the equilibrium: Grossular + clinochlore = 3 diopside + 2 spinel + 4 H_2O. Canadian Mineralogist, 26, 269–281.

Wones, D.R., and Dodge, F.C.W. (1977) The stability of phlogopite in the presence of quartz and diopside. In. D.G. Fraser, Ed., Thermodynamics in geology, p. 229–247, Reidel, Dordrecht.

Wood, B.J. (1979) Activity-composition relationships in Ca(Mg,Fe)Si_2O_6-$CaAl_2SiO_6$ clinopyroxene solid solutions. American Journal of Science, 279, 854–875.

Manuscript received January 30, 1990
Manuscript accepted February 14, 1991